
Doctoral Dissertations

Student Theses and Dissertations

1966

The anodic behavior of zinc in aqueous salt solutions

Yun-chung Sun

Follow this and additional works at: https://scholarsmine.mst.edu/doctoral_dissertations



Part of the [Chemical Engineering Commons](#)

Department: **Chemical and Biochemical Engineering**

Recommended Citation

Sun, Yun-chung, "The anodic behavior of zinc in aqueous salt solutions" (1966). *Doctoral Dissertations*. 448.

https://scholarsmine.mst.edu/doctoral_dissertations/448

This thesis is brought to you by Scholars' Mine, a service of the Missouri S&T Library and Learning Resources. This work is protected by U. S. Copyright Law. Unauthorized use including reproduction for redistribution requires the permission of the copyright holder. For more information, please contact scholarsmine@mst.edu.

THE ANODIC BEHAVIOR OF ZINC IN
AQUEOUS SALT SOLUTIONS

A Dissertation
Presented to
the Faculty of the Graduate School
University of Missouri at Rolla

In Partial Fulfillment
of the Requirements for the Degree
Doctor of Philosophy

by
Yun-chung Sun
June 1966

The author is deeply indebted to Dr. James W. Johnson, Associate Professor of Chemical Engineering and Research Associate in the Graduate Center for Materials Research and to Dr. William J. James, Professor of Chemistry and Director of the Graduate Center for serving as research advisors. Their help, guidance, and encouragement are sincerely appreciated. He would also like to express his thanks to Dr. Martin E. Straumanis, Professor of Metallurgical Engineering and Research Professor of Materials, for his assistance on several occasions.

Thanks are extended to the Graduate Center of the University of Missouri Space Sciences Research Center for the use of its equipment and facilities.

He gratefully acknowledges the graduate research assistantship given by the Center which enabled him to study at this school.

CHAPTER	PAGE
I. INTRODUCTION	1
II. LITERATURE REVIEW	3
III. EXPERIMENTAL	18
The Effect of Concentration, Current Density, and Temperature on the Apparent Valence of Zinc Undergoing Anodic Dissolution in KNO_3 - K_2SO_4 Solutions	18
Apparatus	18
Procedure	19
Sample Calculations	23
Data and Results	25
The Anodic Potential-Current Density Relationship for the Anodic Dissolution of Zinc in KNO_3 - K_2SO_4 Solutions	29
Apparatus	29
Procedure	29
Sample Calculations	29
Data and Results	30
Effect of Zinc Salt Solutions on Apparent Valence of Zinc Undergoing Anodic Dissolution ...	30
Apparatus	30
Procedure	30
Sample Calculations	32
Data and Results	32

The Anodic Potential-Current Density	
Relationship for the Anodic Dissolution of	
Zinc in Zinc Salt Solutions	32
Apparatus	32
Procedure	32
Data and Results	32
IV. DISCUSSION	35
V. RECOMMENDATIONS	59
VI. LIMITATIONS	60
VII. SUMMARY AND CONCLUSIONS	61
BIBLIOGRAPHY	63
Appendix A. Materials	68
Appendix B. Apparatus	70
Appendix C. Miscellaneous Experimental Procedure	72
Appendix D. Experimental Data	75
VITA	114

TABLE	PAGE
I. Apparent Valence of Zinc Dissolving Anodically in 0.30 M K_2SO_4 Solution at 25°C .	76
II. Apparent Valence of Zinc Dissolving Anodically in 0.050 M KNO_3 +0.317 M K_2SO_4 Solution at 25°C	76
III. Apparent Valence of Zinc Dissolving Anodically in 0.10 M KNO_3 +0.30 M K_2SO_4 Solution at 25°C	77
IV. Apparent Valence of Zinc Dissolving Anodically in 0.30 M KNO_3 +0.233 M K_2SO_4 Solution at 25°C	77
V. Apparent Valence of Zinc Dissolving Anodically in 0.50 M KNO_3 +0.167 M K_2SO_4 Solution at 25°C	78
VI. Apparent Valence of Zinc Dissolving Anodically in 0.70 M KNO_3 +0.10 M K_2SO_4 Solution at 25°C	78
VII. Apparent Valence of Zinc Dissolving Anodically in 1.0 M KNO_3 Solution at 25°C ...	79
VIII. Apparent Valence of Zinc Dissolving Anodically in 2.0 M KNO_3 Solution at 25°C ...	79
IX. Apparent Valence of Zinc Dissolving Anodically in 0.050 M KNO_3 +0.317 M K_2SO_4 Solution at 40°C	80

X.	Apparent Valence of Zinc Dissolving Anodically in 0.10 M KNO_3 +0.30 M K_2SO_4 Solution at 40°C	80
XI.	Apparent Valence of Zinc Dissolving Anodically in 0.50 M KNO_3 +0.167 M K_2SO_4 Solution at 40°C	81
XII.	Apparent Valence of Zinc Dissolving Anodically in 1.0 M KNO_3 Solution at 40°C ..	81
XIII.	Apparent Valence of Zinc Dissolving Anodically in 0.050 M KNO_3 +0.317 M K_2SO_4 Solution at 55°C	82
XIV.	Apparent Valence of Zinc Dissolving Anodically in 0.10 M KNO_3 +0.30 M K_2SO_4 Solution at 55°C	82
XV.	Apparent Valence of Zinc Dissolving Anodically in 0.50 M KNO_3 +0.167 M K_2SO_4 Solution at 55°C	83
XVI.	Apparent Valence of Zinc Dissolving Anodically in 1.0 M KNO_3 Solution at 55°C ..	83
XVII.	The Anodic Potential-Current Density Relationship of Zinc Dissolving Anodically in 0.050 M KNO_3 +0.317 M K_2SO_4 Solution at 25°C	84
XVIII.	The Anodic Potential-Current Density Relationship of Zinc Dissolving Anodically in 0.10 M KNO_3 +0.30 M K_2SO_4 Solution at 25°C	84

XIX.	The Anodic Potential-Current Density Relationship of Zinc Dissolving Anodically in 0.50 M KNO_3 +0.167 M K_2SO_4 Solution at 25°C.	85
XX.	The Anodic Potential-Current Density Relationship of Zinc Dissolving Anodically in 1.0 M KNO_3 Solution at 25°C	85
XXI.	The Anodic Potential-Current Density Relationship of Zinc Dissolving Anodically in 0.050 M KNO_3 +0.317 M K_2SO_4 Solution at 40°C	86
XXII.	The Anodic Potential-Current Density Relationship of Zinc Dissolving Anodically in 0.10 M KNO_3 +0.30 M K_2SO_4 Solution at 40°C .	86
XXIII.	The Anodic Potential-Current Density Relationship of Zinc Dissolving Anodically in 0.50 M KNO_3 +0.167 M K_2SO_4 Solution at 40°C	87
XXIV.	The Anodic Potential-Current Density Relationship of Zinc Dissolving Anodically in 1.0 M KNO_3 Solution at 40°C	87
XXV.	The Anodic Potential-Current Density Relationship of Zinc Dissolving Anodically in 0.050 M KNO_3 +0.317 M K_2SO_4 Solution at 55°C	88

XXVI.	The Anodic Potential-Current Density Relationship of Zinc Dissolving Anodically in 0.10 M KNO_3 +0.30 M K_2SO_4 Solution at 55°C	88
XXVII.	The Anodic Potential-Current Density Relationship of Zinc Dissolving Anodically in 0.50 M KNO_3 +0.167 M K_2SO_4 Solution at 55°C	89
XXVIII.	The Anodic Potential-Current Density Relationship of Zinc Dissolving Anodically in 1.0 M KNO_3 Solution at 55°C	89
XXIX.	Apparent Valence of Zinc Dissolving Anodically in 0.23 M K_2SO_4 +0.10 M ZnCl_2 Solution	90
XXX.	Apparent Valence of Zinc Dissolving Anodically in 0.23 M K_2SO_4 +0.10 M ZnBr_2 Solution	90
XXXI.	Apparent Valence of Zinc Dissolving Anodically in 0.23 M K_2SO_4 +0.10 M ZnI_2 Solution	91
XXXII.	Apparent Valence of Zinc Dissolving Anodically in 0.20 M K_2SO_4 +0.10 M ZnSO_4 Solution	91
XXXIII.	Apparent Valence of Zinc Dissolving Anodically in 0.23 M K_2SO_4 +0.10 M $\text{Zn}(\text{C}_2\text{H}_3\text{O}_2)_2$ Solution	92

TABLE	PAGE
XXXIV. Apparent Valence of Zinc Dissolving Anodically in 0.23 M K_2SO_4 +0.10 M $Zn(NO_3)_2$ Solution	92
XXXV. Apparent Valence of Zinc Dissolving Anodically in 0.32 M K_2SO_4 + 0.010 M $ZnCl_2$ Solution	93
XXXVI. Apparent Valence of Zinc Dissolving Anodically in 0.32 M K_2SO_4 +0.010 M $ZnBr_2$ Solution	93
XXXVII. Apparent Valence of Zinc Dissolving Anodically in 0.32 M K_2SO_4 +0.010 M ZnI_2 Solution	94
XXXVIII. Apparent Valence of Zinc Dissolving Anodically in 0.32 M K_2SO_4 +0.010 M $ZnSO_4$ Solution	94
XXXIX. Apparent Valence of Zinc Dissolving Anodically in 0.32 M K_2SO_4 +0.010 M $Zn(C_2H_3O_2)_2$ Solution	95
XL. Apparent Valence of Zinc Dissolving Anodically in 0.32 M K_2SO_4 +0.010 M $Zn(NO_3)_2$ Solution	95
XLI. The Anodic Potential-Current Density Relationship of Zinc Dissolving Anodically in 0.23 M K_2SO_4 +0.10 M $ZnCl_2$ Solution at 25°C	96

TABLE	PAGE
XLII. The Anodic Potential-Current Density Relationship of Zinc Dissolving Anodically in 0.32 M K_2SO_4 +0.010 M $ZnCl_2$ Solution at 25°C	96
XLIII. The Anodic Potential-Current Density Relationship of Zinc Dissolving Anodically in 0.23 M K_2SO_4 +0.10 M $ZnBr_2$ Solution at 25°C	97
XLIV. The Anodic Potential-Current Density Relationship of Zinc Dissolving Anodically in 0.32 M K_2SO_4 +0.010 M $ZnBr_2$ Solution at 25°C	97
XLV. The Anodic Potential-Current Density Relationship of Zinc Dissolving Anodically in 0.23 M K_2SO_4 +0.10 M ZnI_2 Solution at 25°C	98
XLVI. The Anodic Potential-Current Density Relationship of Zinc Dissolving Anodically in 0.32 M K_2SO_4 +0.010 M ZnI_2 Solution at 25°C	98
XLVII. The Anodic Potential-Current Density Relationship of Zinc Dissolving Anodically in 0.20 M K_2SO_4 +0.10 M $ZnSO_4$ Solution at 25°C	99

TABLE

PAGE

XLVIII.	The Anodic Potential-Current Density Relationship of Zinc Dissolving Anodically in 0.32 M K_2SO_4 +0.010 M $ZnSO_4$ Solution at 25°C	99
IL.	The Anodic Potential-Current Density Relationship of Zinc Dissolving Anodically in 0.23 M K_2SO_4 +0.10 M $Zn(C_2H_3O_2)_2$ Solution at 25°C	100
L.	The Anodic Potential-Current Density Relationship of Zinc Dissolving Anodically in 0.32 M K_2SO_4 +0.010 M $Zn(C_2H_3O_2)_2$ Solution at 25°C	100
LI.	The Anodic Potential-Current Density Relationship of Zinc Dissolving Anodically in 0.23 M K_2SO_4 +0.10 M $Zn(NO_3)_2$ Solution at 25°C	101
LII.	The Anodic Potential-Current Density Relationship of Zinc Dissolving Anodically in 0.32 M K_2SO_4 +0.010 M $Zn(NO_3)_2$ Solution at 25°C	101
LIII.	The Anodic Potential-Current Density Relationship of Zinc Dissolving Anodically in 0.23 M K_2SO_4 +0.10 M $ZnCl_2$ Solution at 40°C	102

LX.	The Anodic Potential-Current Density Relationship of Zinc Dissolving Anodically in 0.32 M K_2SO_4 +0.010 M $ZnSO_4$ Solution at 40°C	105
LXI.	The Anodic Potential-Current Density Relationship of Zinc Dissolving Anodically in 0.23 M K_2SO_4 +0.10 M $Zn(C_2H_3O_2)_2$ Solution at 40°C	106
LXII.	The Anodic Potential-Current Density Relationship of Zinc Dissolving Anodically in 0.32 M K_2SO_4 +0.010 M $Zn(C_2H_3O_2)_2$ Solution at 40°C	106
LXIII.	The Anodic Potential-Current Density Relationship of Zinc Dissolving Anodically in 0.23 M K_2SO_4 +0.10 M $Zn(NO_3)_2$ Solution at 40°C	107
LXIV.	The Anodic Potential-Current Density Relationship of Zinc Dissolving Anodically in 0.32 M K_2SO_4 +0.010 M $Zn(NO_3)_2$ Solution at 40°C	107
LXV.	The Anodic Potential-Current Density Relationship of Zinc Dissolving Anodically in 0.23 M K_2SO_4 +0.10 M $ZnCl_2$ Solution at 55°C	108

TABLE	PAGE
LXVI. The Anodic Potential-Current Density Relationship of Zinc Dissolving Anodically in 0.32 M K_2SO_4 +0.010 M $ZnCl_2$ Solution at 55°C	108
LXVII. The Anodic Potential-Current Density Relationship of Zinc Dissolving Anodically in 0.23 M K_2SO_4 +0.10 M $ZnBr_2$ Solution at 55°C	109
LXVIII. The Anodic Potential-Current Density Relationship of Zinc Dissolving Anodically in 0.32 M K_2SO_4 +0.010 M $ZnBr_2$ Solution at 55°C	109
LXIX. The Anodic Potential-Current Density Relationship of Zinc Dissolving Anodically in 0.23 M K_2SO_4 +0.10 M ZnI_2 Solution at 55°C	110
LXX. The Anodic Potential-Current Density Relationship of Zinc Dissolving Anodically in 0.32 M K_2SO_4 +0.010 M ZnI_2 Solution at 55°C	110
LXXI. The Anodic Potential-Current Density Relationship of Zinc Dissolving Anodically in 0.20 M K_2SO_4 +0.10 M $ZnSO_4$ Solution at 55°C	111

TABLE	PAGE
LXXII. The Anodic Potential-Current Density Relationship of Zinc Dissolving Anodically in 0.32 M K_2SO_4 +0.010 M $ZnSO_4$ Solution at 55°C	111
LXXIII. The Anodic Potential-Current Density Relationship of Zinc Dissolving Anodically in 0.23 M K_2SO_4 +0.10 M $Zn(C_2H_3O_2)_2$ Solution at 55°C	112
LXXIV. The Anodic Potential-Current Density Relationship of Zinc Dissolving Anodically in 0.32 M K_2SO_4 +0.010 M $Zn(C_2H_3O_2)_2$ Solution at 55°C	112
LXXV. The Anodic Potential-Current Density Relationship of Zinc Dissolving Anodically in 0.23 M K_2SO_4 +0.10 M $Zn(NO_3)_2$ Solution at 55°C	113
LXXVI. The Anodic Potential-Current Density Relationship of Zinc Dissolving Anodically in 0.32 M K_2SO_4 +0.010 M $Zn(NO_3)_2$ Solution at 55°C	113

LIST OF FIGURES

FIGURE	PAGE
1. The Electrolysis Cell	20
2. The Arrangement of Experimental Apparatus	21
3. The Electrode	22
4. Apparent Valence of Zinc Undergoing Anodic Dissolution in $\text{KNO}_3\text{-K}_2\text{SO}_4$ Solution (ionic strength = 1.0) at 25°C	26
5. Apparent Valence of Zinc Undergoing Anodic Dissolution in $\text{KNO}_3\text{-K}_2\text{SO}_4$ Solution (ionic strength = 1.0) at 40°C	27
6. Apparent Valence of Zinc Undergoing Anodic Dissolution in $\text{KNO}_3\text{-K}_2\text{SO}_4$ Solution (ionic strength = 1.0) at 55°C	28
7. Tafel Plot for the Anodic Dissolution of Zinc in $\text{KNO}_3\text{-K}_2\text{SO}_4$ Solution (ionic strength = 1.0) at 25°C	31
8. Tafel Plot for the Anodic Dissolution of Zinc in $\text{ZnSO}_4\text{-K}_2\text{SO}_4$ Solution (ionic strength = 1.0) at 25°C	34
9. The Effect of Nitrate Ion Concentration on the Apparent Valence of Zinc Undergoing Anodic Dissolution at 25°C	39
10. The Effect of Nitrate Ion Concentration on the Apparent Valence of Zinc Undergoing Anodic Dissolution at 40°C	40

FIGURE	PAGE
11. The Effect of Nitrate Ion Concentration on the Apparent Valence of Zinc Undergoing Anodic Dissolution at 55°C	41
12. The Effect of Current Density on the Apparent Valence of Zinc Undergoing Anodic Dissolution at 25°C	42
13. The Effect of Current Density on the Apparent Valence of Zinc Undergoing Anodic Dissolution at 40°C	43
14. The Effect of Current Density on the Apparent Valence of Zinc Undergoing Anodic Dissolution at 55°C	44
15. The Effect of Temperature on the Apparent Valence of Zinc Undergoing Anodic Dissolution..	46
16. The Effect of Temperature on the Apparent Valence of Zinc Undergoing Anodic Dissolution..	49

CHAPTER I

INTRODUCTION

The increasing demand for protective metals as coatings and non-corrosive alloys has caused extensive research on the fundamental behavior of metals in corrosive media. The problem of controlling the destructive process of metallic corrosion still exists and becomes urgent in this space age. The desirability of metals such as beryllium, magnesium, and zinc in air frame and space structural units, because of their high strength to weight ratio, has been responsible for the considerable progress in their technology in recent years.

The basic mechanism of the anodic dissolution of metals such as zinc, cadmium, and magnesium in salt solution is not completely known. Many mechanisms have been proposed by different investigators but evidence is still lacking which would allow one to draw reliable conclusions and to explain the discrepancies which often arise between coulometric data and the weight loss of the metal electrodes in certain salt solutions.

The study of the influence of anions as well as cations on the anodic behavior of zinc undergoing dissolution might give an insight into the basic mechanism of metallic corrosion and the type of substances needed for corrosion inhibition.

The purpose of this investigation was to obtain a mechanism for the anodic dissolution of zinc that would relate the rate of dissolution, the anodic current density, the influence of anions, and other parameters to the observed behavior.

CHAPTER II

LITERATURE REVIEW

This literature review traces the development of different mechanisms proposed by other investigators in explaining the abnormal anodic dissolution of metals. Since several metals other than zinc have been studied, from this view point, it is proper to include such information in order to give a general picture of the anodic dissolution of metals in aqueous solutions. For this reason, the literature reports of the anodic behavior of cadmium, magnesium, beryllium, etc., as well as zinc are presented in this section.

When either zinc or cadmium is dissolved anodically in aqueous salt solutions (neutral), in the absence of oxidizing agents, an oxidation state of two is normally obtained. However, in the presence of certain oxidizing agents such as nitrate ions, the number of coulombs required to dissolve one gram-equivalent weight of these metals is always less than the amount calculated using Faraday's law assuming a normal valence of two. This abnormality has been investigated and several mechanisms have been proposed.

In the early twentieth century, colloidal solutions of metals were found in the vicinity of anodes (platinum, gold, silver, bismuth, lead, and iron) during electrolysis of pure water (1). In 1906, Burton (2) observed that

clouds of tiny metallic particles scattered from the cathode during sparking and remained suspended in the water for a time depending on the nature of the metals. He used a storage battery capable of providing voltages up to 110 volts and controlled the current with a variable resistance in series with the electrolysis cell. Normally, 30 to 60 volts and currents of 6.5 to 7.5 amperes were used to produce the colloidal solutions. The mechanism of the process was described as the vaporization of the metal at the electrode during electrolysis followed by dispersion and condensation of the metal vapor in the solution.

White (3) reported in 1911, that the "percentage current efficiency" of cadmium undergoing anodic dissolution in aqueous nitrate solution was often larger than 100 percent assuming a normal valence of two. Using the same method, he found that the current efficiency for the zinc anode was approximately 100 percent in most aqueous electrolytes. His results were by no means reproducible as the current efficiency ranged from 80.0 to 109.8 percent in five trials. The main reason for this anomalous result is believed to have been due to an incomplete removal of the film formed on the anode during electrolysis.

Later on, Del Boca (4) proposed a mechanism for zinc and cadmium undergoing anodic dissolution in liquid NH_3 . He suggested that a portion of the anode was dissolved as

atoms and transported to the cathode through the solution either by electrophoresis or by attachment to the divalent ions as $M.M^{++}$.

In 1955, Epelboin (5) reported an apparent valence of 1.40 for the anodic dissolution of zinc in the presence of perchlorate ions. The values were obtained by both weighing the zinc electrode after electrolysis and determining the amount of chloride ion formed from the reduction of the perchlorate ion. This mechanism sometimes referred to as the "uncommon valency" model has received considerable support, in particular from the studies of Davidson, Kleinberg, and Sorensen (6-9). They calculated the initial mean valence number of several active metals undergoing anodic dissolution in different electrolytes. The electrolytic cell was connected in series with a variable voltage full-wave mercury tube rectifier, a silver coulometer, and an ammeter. The initial valence number, V_i , of the metallic ions formed was calculated from the equation:

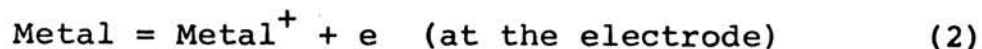
$$V_i = \frac{(\text{Wt. of silver deposited in coulometer}) (\text{At. Wt. of metal})}{(107.88) (\text{Wt. of metal lost from anode})}$$

(1)

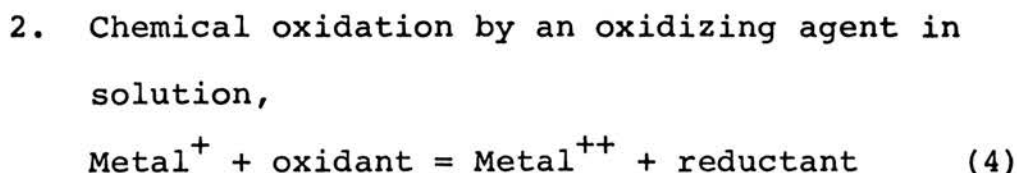
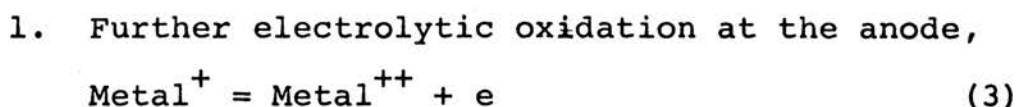
The value of V_i for cadmium dissolving in 0.20 M NaNO_3 solution at 30°C was found to be 1.55. It decreased linearly with increasing temperature. The value of V_i for zinc dissolving in 3 percent KNO_3 solution was found

to be about 1.87 at room temperature and it decreased linearly with increasing temperature. Cadmium showed an initial mean valence of two in NaCl, KCl, and KClO₃ solutions. In the latter medium, however, zinc had an initial mean valence of less than two.

The results were explained on the hypothesis that the primary reaction at the metal anode consisted of a stepwise oxidation. The first step was the oxidation of the metal to the unipositive ion:



The unipositive ion would be expected to be very unstable and would readily form the normal bipositive ion as the second step. This second step could be either one of two reactions:

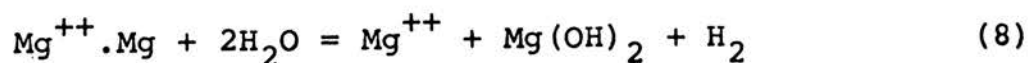
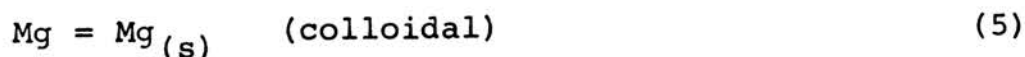


In nonreducible electrolytes, reaction (4) could not occur, and consequently an initial mean valence of two would be found. In reducible electrolytes, the two possible mechanisms would be competitive. The step which predominates would depend on the nature of the oxidizing electrolyte and the conditions of the experiment. Thus, the initial mean valence might range from plus one to two, depending upon the relative extents of reaction (3) and

(4). Reaction (4) would be expected to increase with increasing concentration of the oxidant. An analysis at the end of the run carried out in 3 percent NaNO_3 using a cadmium anode revealed the presence of nitrite ions, thus illustrating the reducing power of some corrosion product, assumed to be unipositive ions. Attempts to qualitatively detect the presence of these ions were unsuccessful. The formation of a gray-black film on the surface of the zinc anode during electrolysis in NaNO_3 was reported but no further mention was made of its possible importance. No attempt was made to explain the anomalous behavior of cadmium in chlorate solutions.

In 1958, using x-ray diffraction analysis, Hoey and Cohen (10) indentified a film of $\text{Mg}(\text{OH})_2$, MgO , and Mg which formed at the surface of a magnesium anode during anodic and cathodic polarization in 110 ppm NaCl solution. They further observed magnesium metal particles in the film with a microscope.

In the proposed mechanism for the anodic oxidation of magnesium, the following reactions were suggested as being energetically possible:



The formation of $\text{Mg}^{++}.\text{Mg}$ or colloidal magnesium (Mg_s) in equations (5) and (6) was attributed to undermined

magnesium which was detached from the electrode during electrolysis. Reaction (7) corresponded to cathodic local corrosion at the anode. Reaction (8) was given as the possible source of $Mg(OH)_2$ on the electrode and in the electrolyte.

More recently, Marsh and Schaschl (11) suggested that when steel dissolves anodically at a high rate, the corrosion proceeds by removal of "chunks of iron" containing several atoms. Because of this expulsion of metallic particles, the metal does not dissolve as predicted by Faraday's law.

Robinson and King (12) have concluded that the electrochemical behavior of magnesium can be satisfactorily explained on the basis of normal valence ion formation. The hydroxide film on the surface in aqueous environments is extremely protective, but is responsive to electrochemical and environmental changes. This has led to a "film-controlled" theory for some light metals undergoing anodic dissolution as a means of explaining their abnormal behavior.

Another mechanism suggested by Greenblatt (13) for the anodic dissolution of magnesium was that as magnesium ions leave the metal lattice, a finite time is required for them to diffuse through an oxide film, thus creating an excess of positive ions. The film with excess positive ions must also have an equal number of anion vacancies. To obtain electrical neutrality, electrons flow across the

film filling the anion vacancies and therefore do not pass through the external circuit. Thus, the amount of current measured in the external circuit is deficient due to this flow of electrons through the film. This results in a greater amount of metal being dissolved than the number of coulombs passed through the external circuit would indicate.

Later, Straumanis and Mathis (14) confirmed the disintegration of beryllium metal using optical methods with high magnification. They observed a large number of deformation twins in the metallic residue collected in the anolyte. Similar twins were present on etched surfaces of the beryllium metal. Since deformation twins arise in the castings from stresses set up due to temperature gradients and do not occur in nucleation from aqueous media, their studies provided conclusive proof of the origin of the particles.

Straumanis and Bhatia (15) showed also that magnesium disintegrated partially into very small metallic particles under certain conditions of dissolution or corrosion. The dark-gray color of the film separating from the anode during electrolysis was caused by the presence of tiny magnesium particles (some deformation twins were present) held in a matrix of $Mg(OH)_2$ as confirmed with a high magnification microscope employing both reflected and transmitted light.

According to Evans (16), "anodic corrosion eats its way along grain boundaries, so that the grains themselves drop out unchanged, causing a weight-loss greater than the calculated value." This grain dropout is, however, not to be confused with what is termed anodic disintegration. Stoner (17) and Wang (18) employing single crystals of zinc and Daniels (19) using single crystals of magnesium have shown that disintegration occurs on oriented samples. Furthermore disintegration of single grains are evident on microscopic examination of polycrystalline magnesium and beryllium. There is evidence, however, that some large chunks of beryllium metal in the anolyte arise from a preferential attack at grain boundaries and impure beryllium appears qualitatively to form larger quantities of undissolved beryllium particles than does pure beryllium during anodic dissolution in aqueous sodium chloride.

Another electrochemical phenomenon which has been related to the uncommon valence of metals undergoing anodic dissolution is called the "difference effect". This was first recognized and named by Thiel and Eckell (20) and is given by the equation $\Delta = V_1 - V_2$, where V_1 is the hydrogen evolution rate from an electrode without current flowing and V_2 is the rate from the same electrode with current flowing. They studied the dissolution of zinc in dilute acid solution and later on the dissolution of aluminum in sodium hydroxide solutions. In their

experiments with aluminum at a given temperature and concentration of electrolyte, the metal dissolved freely at a rate V_1 , as measured by hydrogen evolution. When the same experiment was repeated with the aluminum specimen connected to a more noble electrode immersed in the same solution, the rate of hydrogen evolution V_2 was found to be larger than V_1 . They reasoned that when a metal is made an anode in an electrolytic cell, its rate of corrosion (dissolution) should be the sum of: (1) the rate of local corrosion as observed in the absence of the external current, and (2) the corrosion rate equivalent to the external current. In experimental work with metals, however, they found the actual corrosion rate to be less or more than the sum of the components. This deviation was given the name "difference effect". The difference effect can be positive or negative depending on the system. The negative difference effect has been attributed by some investigators to uncommon valence (19).

The positive difference effect has been explained by Straumanis (21) in terms of anodic polarization. He believes that it is more pronounced if there is an interference with the delivery of electrons at the local elements or with the ejection of ions within the interface of the metal anode and the corrosive media. Thus, with increasing anodic current, whether in local elements or externally applied, there will be increasing anodic

polarization. This decreases the driving force for local dissolution and gives rise to the positive difference effect.

Straumanis (22) also explained both the positive and negative difference effects by using the concept of local currents. Two mechanisms were postulated in the general equation suggested for both the positive and negative difference effects: (1) under the influence of the external current produced by the local elements, the local anodes are polarized to more noble values, and (2) film stripping or disruption occurs when the current of local elements is introduced in addition to the external current. The latter mechanism was believed to be due to the ejection of the metal ions, which forced the surface film from the anode and uncovered additional cathodic sites.

A report of both positive and negative difference effects for magnesium dissolving in the same acid was made by James, et al. (23). They reported a linear relationship between Δ and I (current density) only at low current densities. The deviation from linearity became more pronounced with increasing current density and decreasing acid concentration. They proposed that for magnesium dissolving in acids, the difference effect results from: (1) the change in electrochemical conditions at the interface (polarization of local element) which an anodic current is flowing, (2) the ease with which a protective

surface film is formed or disrupted, and (3) the rate at which metallic particles separate from the anode surface.

Kirkov (24) measured the anodic potential of single and polycrystalline zinc electrodes in systems of 1,4-dioxane-water-zinc sulfate, ethanol-water-zinc sulfate, and acetone-water-zinc sulfate. Some relation between the change of the electrode potential and the structural changes in the liquid phase was observed, but no proportionality could be shown between the electrode potential and the content of organic compound in the mixture. The anodic potential deviation from the theoretically predicted value was different at equal electrolyte concentrations for each kind of electrode used. The anodic potentials obtained for various $ZnSO_4$ concentrations deviated considerably from the theoretical values. He reasoned that the standard potential depends on the energy of the surface and the structure of the solvent.

Recently, James, et al. (17,25,26) reported that during electrolysis in potassium nitrate, a gray film formed on the surface of zinc and cadmium anodes. This film was not present in either potassium chloride or potassium sulfate solutions. It was suspected that this film was associated with the abnormal behavior of the anodic dissolution. Amalgamated cadmium and zinc electrodes were used at the suggestion of Hoar (27). He pointed out that amalgamation could prevent the formation

of films such as are observed on zinc and cadmium electrodes in nitrate solutions and might prevent the disintegration of the electrode. As the diffusion of cadmium and zinc ions of any valence should not be prevented by the amalgamation, one might expect the behavior of zinc and cadmium amalgams to be the same as that of zinc and cadmium in the same electrolyte as regards the initial mean valence. The experimental results showed agreement between the faradaic equivalent obtained from the current based on bipovalent ions and the amount of zinc and cadmium dissolved as determined by EDTA titration. They, therefore, rejected the hypothesis that these metals dissolve as ions of lower valence than normal.

The film formation phenomenon was studied by Kochman (28) a year later. He reported that, during anodic dissolution in 2 N H_2SO_4 solution, zinc was passivated by a dark layer of ZnO mixed with a finely dispersed metallic zinc and that the density decreased until the layer was converted completely into ZnO film.

Recently Yoshino (29) measured the anodic potential of zinc electrodes in aqueous solution at 80°C . He reported that the anions HCO_3^- , NO_3^- , and PO_4^{3-} increased the potential, whereas Cl^- and SO_4^{2-} did not. The increase at high temperature was similar to that at room temperature.

Several reports of the influence of anions and cations on the anodic behavior of zinc were made by

Krochmal, et al. (30-32) Solutions of KOH, KCl, and KNO_3 were electrolyzed. The electrical conductivity of KCl and KNO_3 solutions increased after electrolysis. They concluded from the experiments that the composition of the anodic deposits depends on the nature of the anion. They also studied the activity of zinc (99.99 percent) in 0.1 M aqueous HCl solutions containing additions of K_2CO_3 , KClO_3 , K_3PO_4 , K_2HPO_4 , and KH_2PO_4 at 0-4.2 v. All these substances increased the activity of the zinc anode. K_3PO_4 was the most effective. They also reported that the potential of the zinc anode before electrolysis depended on the kind of cations involved, the effect of which decreased in the order $\text{Zn} > \text{Mg} > \text{Na} > \text{NH}_4$.

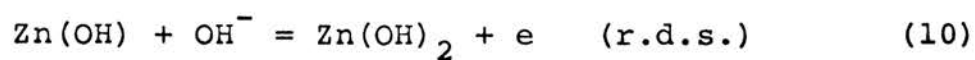
Later, Flerov (33) reasoned that the various states of valency for zinc undergoing anodic dissolution arise because of the electron interaction of the compound on the anode surface. The ionic conductivity in the vicinity of oxide layers on the anode is decreased as is the contact between the active anion and the electrode. The change of valence depended on the ionic conductivity of oxide layers, destruction of the electrode contact with active anions, and spontaneous formation on the electrode of an inactive oxide (hydroxide) modification of the electrode.

In 1964, Uhlig and Krutenat (34) reported work on the determination of the reducing properties of the anolyte and the half-life of the reducing species formed by

anodically polarizing magnesium in 0.1 N NaCl. They confirmed that a reducing species was produced during anodic dissolution of magnesium and that it had a very short period of existence. They concluded that the reducing properties were presumably due to $H^{\circ}(aq)$ and not to an unusual valence magnesium ion. The atomic hydrogen could have been produced either by local cathodic action during exposure of the corroding magnesium anode to the electrolyte or by the reaction of Mg^{+} with H_2O . There is a possibility that the reaction of colloidal magnesium (disintegration products) could also have been the source of $H^{\circ}(aq)$. In such an event the complete reaction of the colloidal magnesium with H_2O would have to be very fast in order to account for an observed half-life of the $H^{\circ}(aq)$ of six minutes. The ionic reaction involving Mg^{+} could conceivably be rapid enough to account for the half-life. They stated that the possible formation of Mg^{+} during anodic dissolution of Mg deserved further study.

In 1963, Chang, Li, and Shieh (35) reported the stationary potentials of a zinc electrode in KOH solution. Anodic polarization curves prepared from data in 1.07-8.31 N KOH solutions showed a linear portion with a slope of 40 mv. At constant current density, the anodic potential shifted 80 mv per pH unit. The corrosion rates in 1.61-9.81 N KOH were determined by a gravimetric method. Log-log plots of i_c versus a_{KOH} showed a linear relation

with a slope of 0.4. On the basis of the results, the mechanism was suggested as:



Thus, the self-dissolution of the zinc electrode in KOH solution could be controlled by either of two competing steps, reaction (10) or the evolution of H_2 at local cathodes.

CHAPTER III

EXPERIMENTAL

The experimental plan consisted of the following phases: the effect of concentration, current density, and temperature on the apparent valence of zinc undergoing anodic dissolution in nitrate-sulfate solution; the anodic potential-current density relationship for the anodic dissolution of zinc in nitrate-sulfate solution; the effect of zinc salts on the apparent valence of zinc undergoing anodic dissolution; and the anodic potential-current density relationship for the anodic dissolution of zinc in zinc salt solutions.

The description of each phase will include apparatus, method of procedure, data and results, and sample calculations.

The materials and apparatus used in this experiment are described in Appendices A and B.

I. THE EFFECT OF CONCENTRATION, CURRENT DENSITY, AND TEMPERATURE ON THE APPARENT VALENCE OF ZINC UNDERGOING ANODIC DISSOLUTION IN $\text{KNO}_3\text{-K}_2\text{SO}_4$ SOLUTIONS

Apparatus. The apparatus consisted of a three compartment electrolytic cell (Figure 1), a constant temperature water bath, a D.C. power supply, a variable resistance box, a milliammeter, a recorder, and an electrometer.

The zinc anode and platinized platinum cathode were connected in series with the power supply, milliammeter, and resistance box. A timer with one tenth second divisions was used to determine the time elapsed during an experiment. A mercurous sulfate electrode was used as the reference electrode. The anodic potential was measured during electrolysis with an electrometer and recorded so that the time variation could be observed (Figure 2). Disodium Ethylenediaminetetraacetate (EDTA) titrations were made to determine the amount of zinc dissolved. Pipettes with capacities of 10 and 25 milliliters were used to withdraw aliquots from the electrolyte. Titrations were made with a micro-burette of 10 milliliter capacity with 0.05 milliliter divisions.

Procedure. A specimen with a cross sectional area of about one square centimeter was cut from a bar of zinc metal of 99.99+ percent purity. A hole whose diameter was slightly less than the zinc specimen was drilled in one end of a teflon bar. A small teflon tube with a copper lead wire was attached to the teflon bar with a screw connection. The metal specimen was then pressed into the teflon mounting so as to provide a gas-tight seal around the metal and to make good electrical contact with the copper wire (Figure 3). The electrode was polished before each run according to the procedure listed in Appendix C. Two hundred milliliters of the electrolyte were transferred

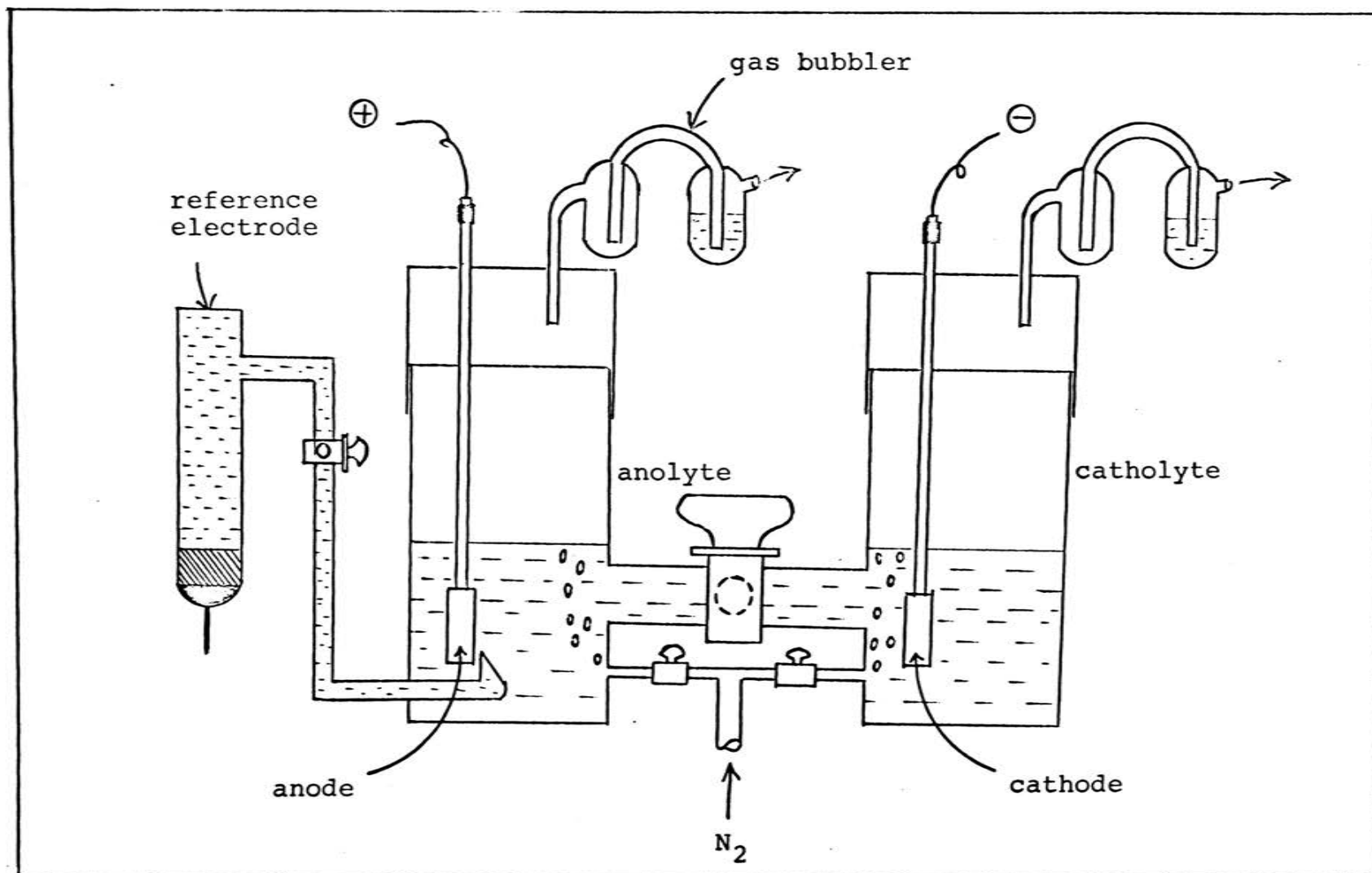


Figure 1. The electrolysis cell.

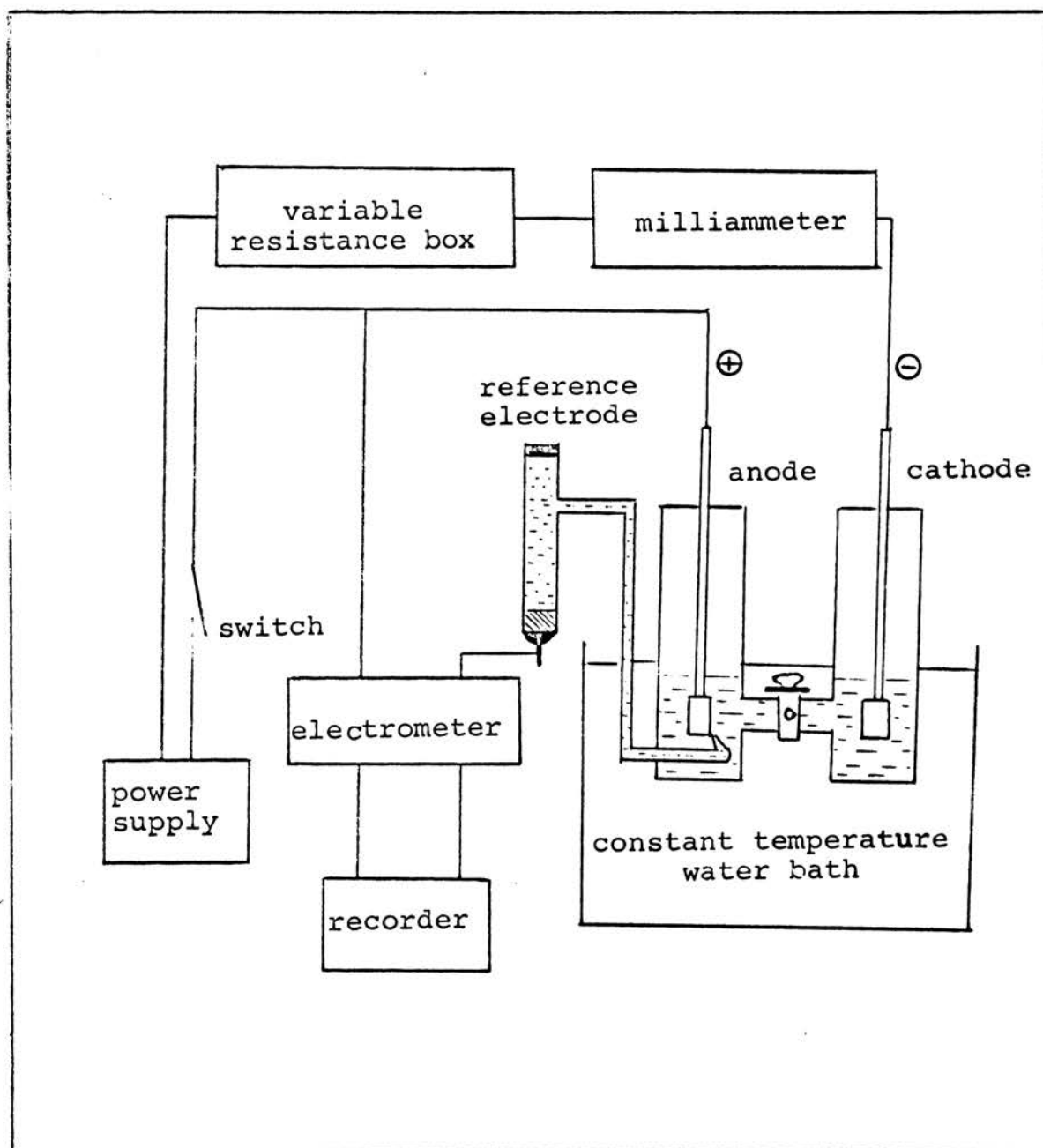


Figure 2. The arrangement of experimental apparatus.

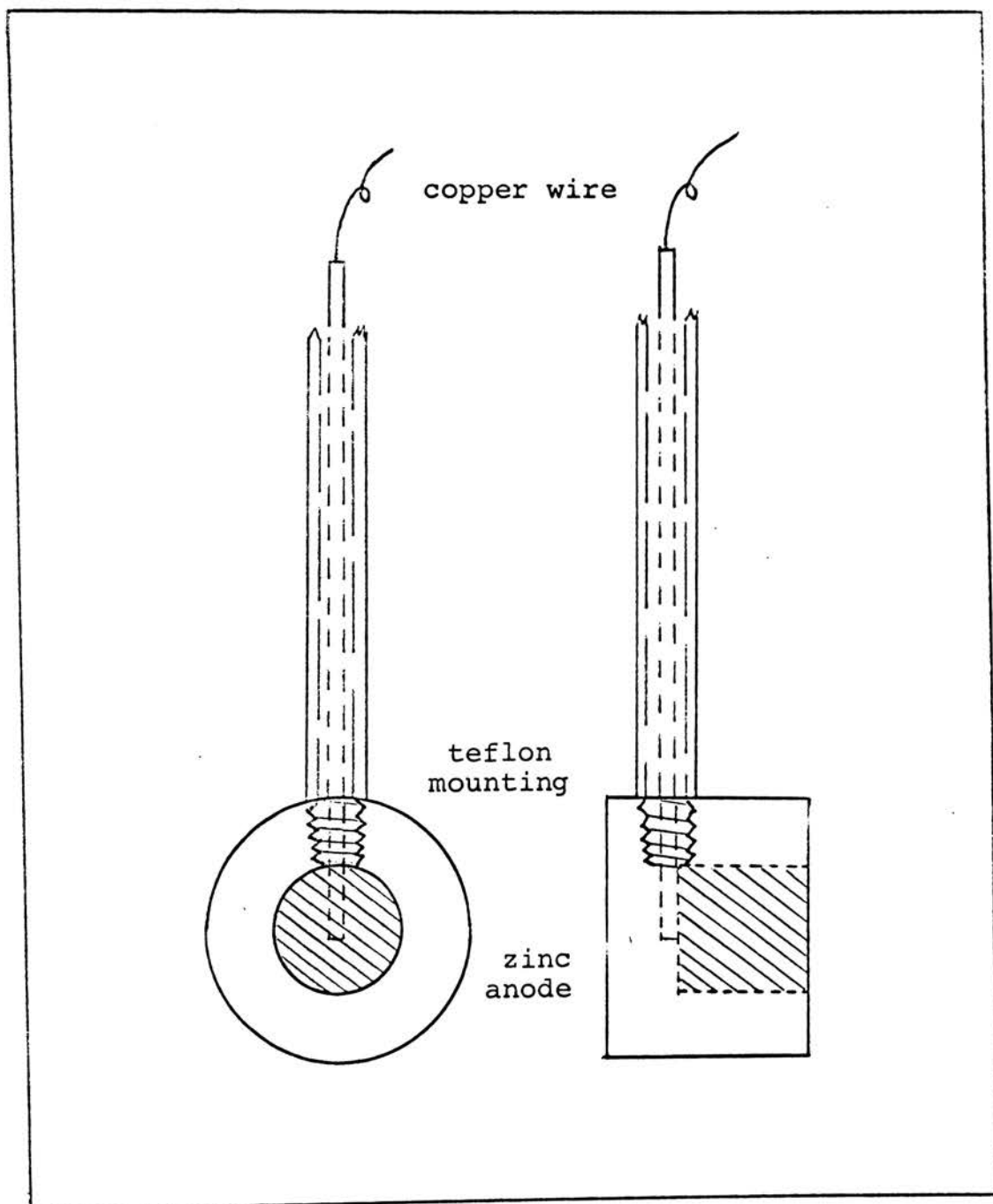


Figure 3. The electrode.

into the electrolytic cell with a 250 milliliter volumetric cylinder. The cell was placed into the constant temperature bath in such a position as to insure complete submergence of the electrolyte. The cell was allowed to remain in the water bath for about 10 to 40 minutes to bring the system to constant temperature before starting a run. The metal anode and the platinum cathode were placed in their respective compartments and nitrogen bubbled through the anolyte and catholyte until a steady anodic potential was reached (approximately a half hour). This served both to flush oxygen from the system and to stir the electrolyte. A run was begun by closing the switch and starting the timer. The current was kept at a steady value by adjusting the decade resistance box. A time ranging from 30 minutes to 18 hours, depending on the current density, was used for an electrolysis run. The time of the run, the current density, and the weight loss of the zinc (determined by EDTA titration) were recorded. The procedure of titration, standardization of EDTA, and the treatment of the white precipitate during electrolysis are described in Appendix C.

Sample Calculations. The method used for calculation of the apparent valence is illustrated using the data for the anodic dissolution of zinc in 0.30 M K_2SO_4 solution at 25°C.

A. Calculation of the apparent weight of zinc dissolved from coulombic data

The apparent weight of zinc dissolved during electrolysis according to Faraday's law, assuming a normal valence of two, was calculated as follows:

$$\text{Weight of zinc (apparent)} = \frac{(I)(t)(\text{atomic weight of zinc})}{(F)(n)}$$

where:

$$I = \text{current} = 0.060 \text{ amp}$$

$$t = \text{time of run} = 1,400 \text{ sec}$$

$$\text{Atomic weight of zinc} = 65.38 \text{ g}$$

$$F = \text{Faraday constant} = 96,500 \text{ amp}\cdot\text{sec/g}\cdot\text{equivalent}$$

$$n = \text{normal cationic charge of zinc} = 2$$

Therefore,

$$\begin{aligned} \text{Weight of zinc (apparent)} &= \frac{(0.060)(1,400)(65.38)}{(96,500)(2)} \\ &= 0.0285 \text{ g} \end{aligned}$$

B. Calculation of the experimental weight of zinc dissolved from EDTA titration

$$\text{Weight of zinc (experimental)} = \frac{(T)(S)(V)}{(A)}$$

where:

$$T = \text{titer value of EDTA} = 0.00163 \text{ g zinc/ml EDTA}$$

$$S = \text{volume of EDTA used} = 1.77 \text{ ml}$$

(average of three titrations)

$$A = \text{volume of aliquot} = 25 \text{ ml}$$

$$V = \text{total volume of electrolyte} = 250 \text{ ml}$$

Therefore,

$$\begin{aligned} \text{Weight of zinc (experimental)} &= \frac{(0.00163)(1.77)(250)}{(25)} \\ &= 0.0289 \text{ g} \end{aligned}$$

C. Calculation of the apparent valence

The apparent valence was calculated by the equation:

$$\begin{aligned} V_i (\text{apparent valence}) &= \frac{(\text{weight of zinc from Faraday's law})(\text{normal valence})}{(\text{weight of zinc experimental})} \\ &= \frac{(0.0285)(2)}{(0.0289)} \\ &= 1.98 \end{aligned}$$

The experimental error was found to be approximately ± 0.03 .

Data and Results. The valence studies were carried out in various potassium nitrate-potassium sulfate solutions at 25, 40, and 55°C. The ionic strength was held constant at one. Various anodic current densities were applied. The results are shown in Figures 4 to 6. The data for each concentration at various current densities are shown in Tables I to XVI of Appendix D. In all cases, the apparent valence decreased with increasing current density and temperature. Below approximately 30 ma/cm², the apparent valence approached the normal valence of two as the current density approached one ma/cm². Above 30 ma/cm², the apparent valence remained approximately constant.

During each run, the current tended to decrease during the first few minutes. This was corrected by adjusting the resistance of the external circuit with the

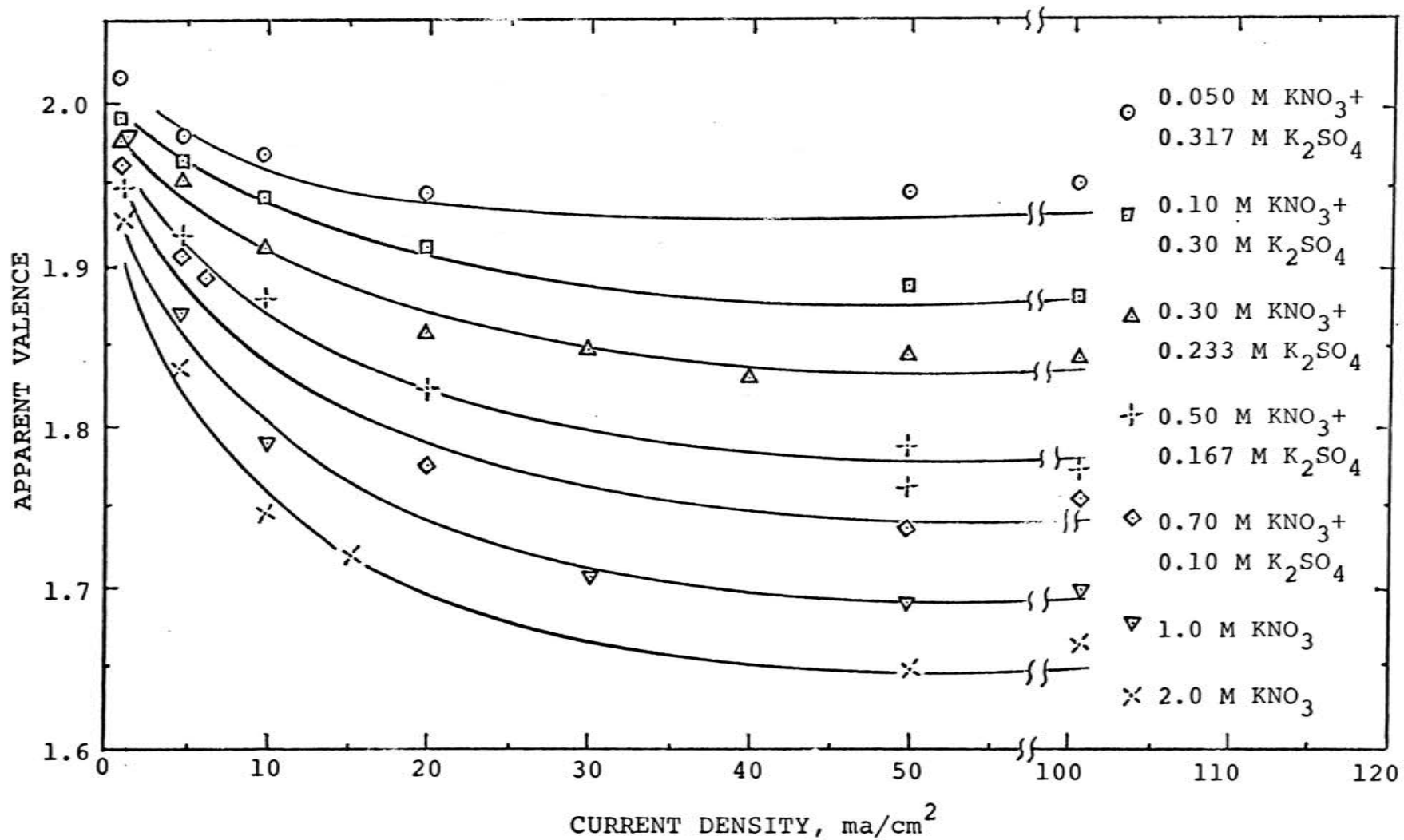


Figure 4. Apparent valence of zinc undergoing anodic dissolution in KNO_3 - K_2SO_4 solution (ionic strength = 1.0) at 25°C .

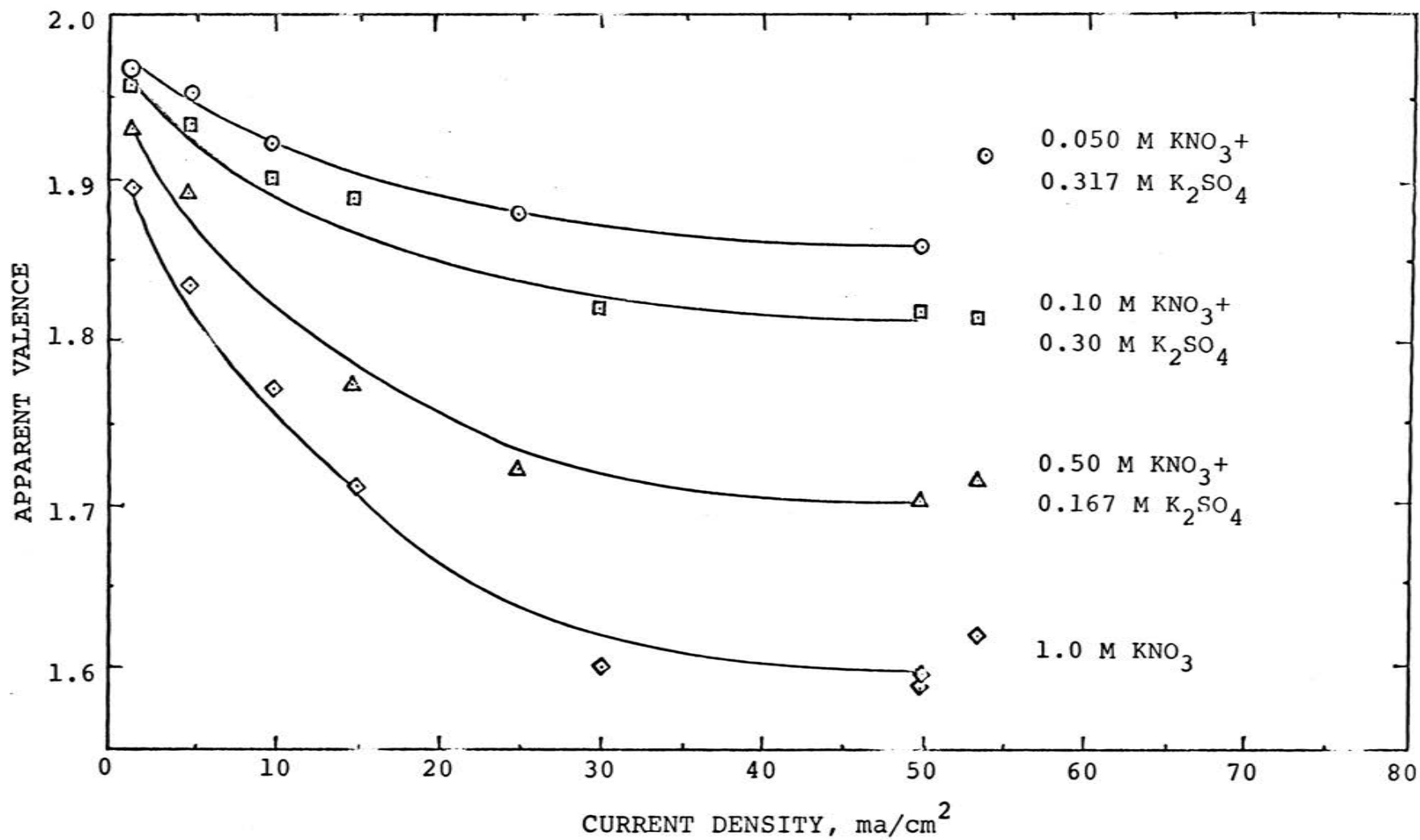


Figure 5. Apparent valence of zinc undergoing anodic dissolution in KNO_3 - K_2SO_4 solution (ionic strength = 1.0) at 40°C .

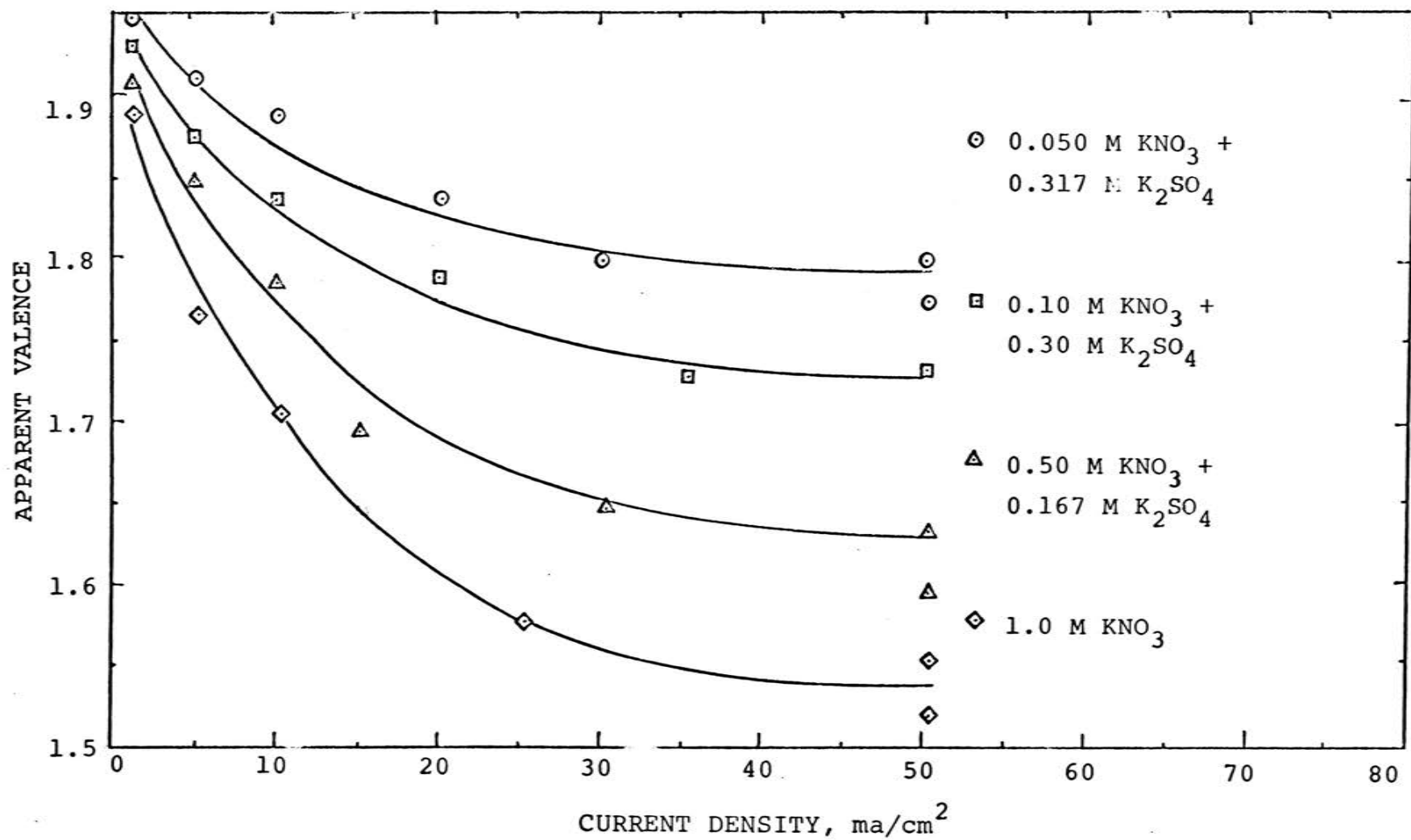


Figure 6. Apparent valence of zinc undergoing anodic dissolution in KNO_3 - K_2SO_4 solution (ionic strength = 1.0) at 55°C .

resistance box. Removal of the zinc anode at the end of a run revealed the presence of a grayish film which turned white after exposure to the air for about five minutes. A white precipitate was observed in the anolyte at a position directly under the zinc anode.

II. THE ANODIC POTENTIAL-CURRENT DENSITY RELATIONSHIP FOR THE ANODIC DISSOLUTION OF ZINC IN KNO_3 - K_2SO_4 SOLUTIONS

Apparatus. The apparatus was the same as described in section I.

Procedure. The procedure was the same as described in section I except the titration was omitted and only sufficient time was allowed at a given current density for the potential to become steady. Current densities ranged from 0.1 to 100 ma/cm^2 . The anodic potential was recorded continuously. Approximately one half hour was necessary to reach a steady value of the anodic potential.

Sample Calculations. The method used for calculation of the anodic potential in this part of experiment is illustrated using the data for the anodic dissolution of zinc in 1.0 M KNO_3 solution at 25°C and at a current density of 0.1 ma/cm^2 .

anodic potential (normal hydrogen scale) =
potential of reference electrode - reading of potentiometer

where:

potential of reference electrode = +0.635 volts
(mercurous sulfate reference electrode, 1 M K_2SO_4)

reading of potentiometer = 1.335 volts

(reading error \pm 0.005 v)

Therefore,

Anodic potential = $+0.635 - 1.335$

= -0.70 volts

Data and Results. The anodic potential-current density studies were carried out at the same electrolyte concentration and temperature as given in the previous section. In all cases, the anodic potential increases with increasing current density. The data are shown in Tables XVII to XXVIII in Appendix D. The results are presented graphically in Figure 7.

III. EFFECT OF ZINC SALT SOLUTIONS ON APPARENT VALENCE OF ZINC UNDERGOING ANODIC DISSOLUTION

Apparatus. The apparatus was the same as described in section I.

Procedure. The same procedure was used as described in section I except the weighing method, described below, was used to determine the amount of zinc dissolved instead of the EDTA titration. Before starting a run, the electrode was polished, rinsed with distilled water, and dried with warm air for approximately ten minutes. The electrode was then weighed on a semi-micro balance with a sensitivity of 0.01 mg. The same drying and weighing procedure was repeated until a constant weight was obtained. Normally, it took approximately thirty minutes to reach constant

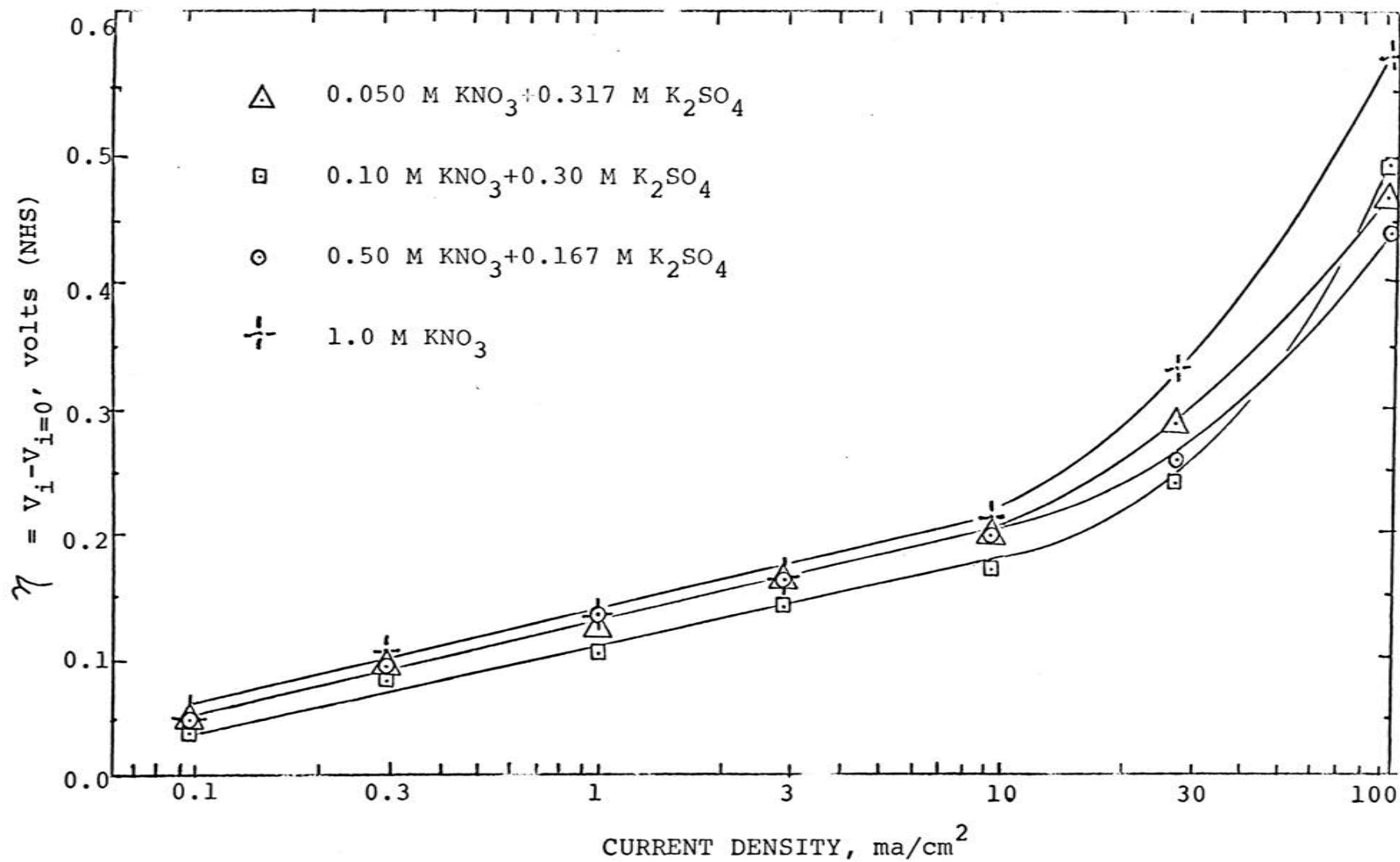


Figure 7. Tafel plot for the anodic dissolution of zinc in KNO_3 - K_2SO_4 solution (ionic strength = 1.0) at 25°C .

weight. The same weighing procedure was used after each electrolysis but the gray films were stripped before weighing.

Sample Calculations. The method used for calculation of the apparent valence was the same as described in section I except the weighing method was used in determining the experimental weight loss of zinc.

Data and Results. The valence studies were carried out in various potassium sulfate-zinc salt (ZnCl_2 , ZnBr_2 , ZnI_2 , ZnSO_4 , $\text{Zn}(\text{C}_2\text{H}_3\text{O}_2)_2$, and $\text{Zn}(\text{NO}_3)_2$) solutions at 25, 40, and 55°C . The ionic strength was held constant at one. Various anodic current densities (1, 10, and 50 ma/cm^2) were applied. The results for each electrolyte concentration at various current densities and temperatures are shown in Tables XXIX to XL in Appendix D.

IV. THE ANODIC POTENTIAL-CURRENT DENSITY RELATIONSHIP FOR THE ANODIC DISSOLUTION OF ZINC IN ZINC SALT SOLUTIONS

Apparatus. The apparatus was the same as described in section I.

Procedure. The same procedure was used as described in section II. It took approximately fifteen minutes to reach a steady value of the anodic potential.

Data and Results. The anodic potential-current density relationship studies were carried out at the same electrolyte concentration and temperature as given in the

previous section. In all cases, the anodic potential increases with increasing current density. The data are shown in Tables XLI to LXXVI in Appendix D. The results are presented graphically in Figure 8.

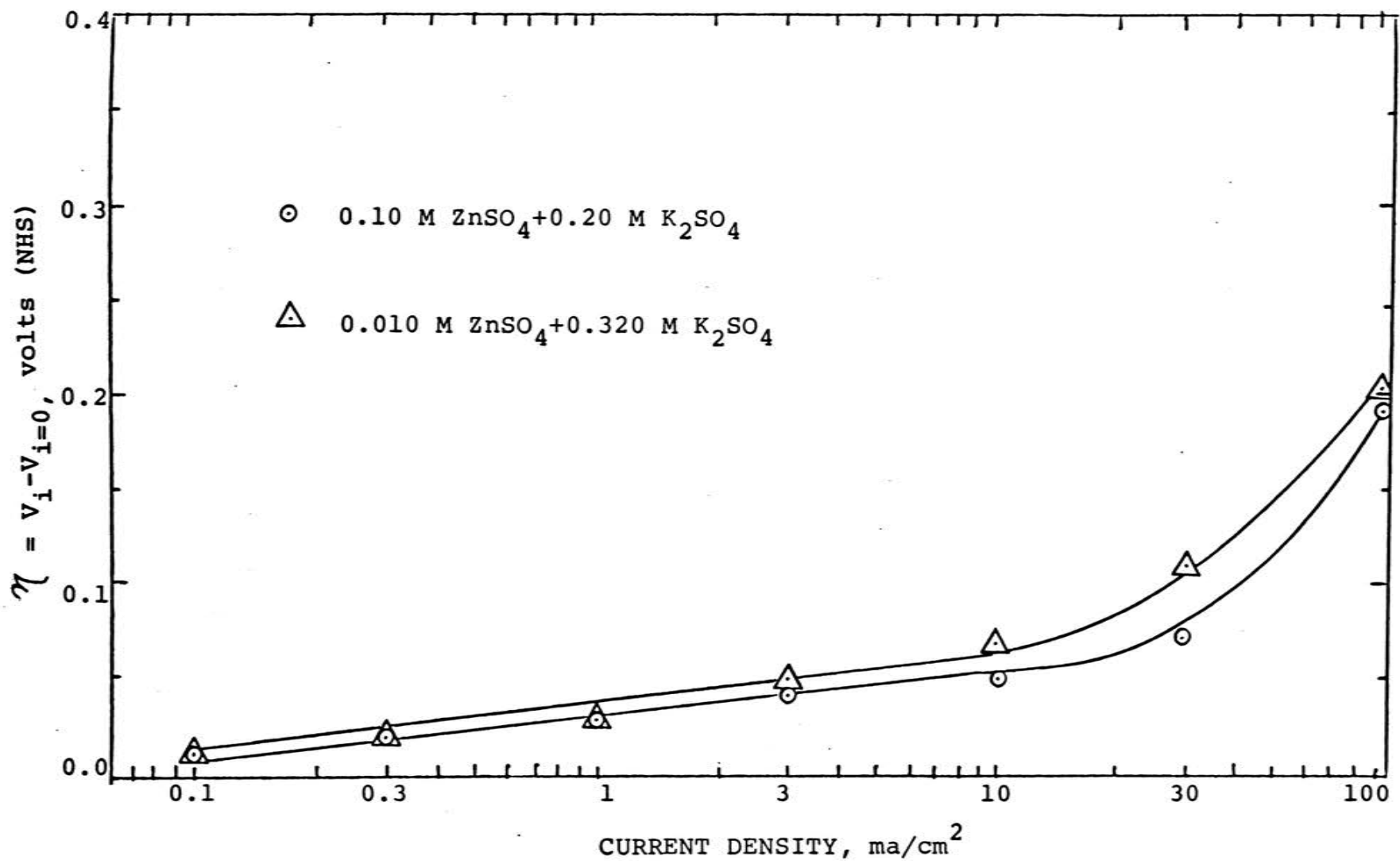


Figure 8. Tafel plot for the anodic dissolution of zinc in ZnSO_4 - K_2SO_4 solution (ionic strength = 1.0) at 25°C.

CHAPTER IV

DISCUSSION

Sorenson, Davidson, and Kleinberg (6-9) have proposed that zinc and cadmium dissolve anodically in certain oxidizing salt solutions with an initial mean valence between one and two.

Recent studies have confirmed that the anodic dissolution of zinc in 3 percent potassium nitrate solution results in valences which are apparently less than two (1.87) at 25°C (17). An apparent valence of 1.46 for cadmium undergoing anodic dissolution in 3 percent potassium nitrate at 25°C was obtained by the author in a previous study (26). These results are consistent with those of Sorenson, et al. (6).

During electrolysis in potassium nitrate solution, a gray film formed on the surface of the zinc anode, but was not formed in either potassium chloride or potassium sulfate solutions. The interesting fact is that this film is present only when electrolysis is performed in certain oxidizing salt solutions where it is also found that the apparent valence is less than two. It was suspected that this film was in some manner associated with the abnormal behavior of the dissolution. As a means of determining the effect of film formation on anodic behavior, Hoar (27) suggested that the dissolution of zinc and cadmium be studied by the use of amalgamated electrodes. The amalgamation might prevent the disintegration of the electrode and the formation of

films such as are observed on the pure metal electrodes in nitrate solution. As the diffusion of metal ions of any valence would not be prevented by the amalgamation, one would expect the behavior of cadmium and zinc amalgams to correspond to that of the metals in the same electrolyte as regards the initial mean valence. Accordingly, amalgamated metal electrodes were prepared and electrolyzed in 3 percent potassium nitrate solution. Values obtained for the mean apparent valence showed agreement between the faradaic equivalence obtained from the current based on bipositive metal ion formation and the amount of metal (Cd or Zn) dissolved as determined by titration with EDTA (17, 26).

The studies carried out with a metal amalgam electrode aroused further interest in the gray corrosion product formed on unamalgamated cadmium and zinc. An x-ray analysis of these films produced diffraction lines for Zn, ZnO, and Zn(OH)₂ when a zinc electrode was used (17) and Cd and Cd(OH)₂ when a cadmium electrode was used (26).

With the view of clarifying some of these previous studies, the work was designed to obtain experimental data for the anodic dissolution of zinc in various concentrations of aqueous nitrate solutions and some other salt solutions as a function of current density and temperature, and to find a relationship in accord with the results. Potentials were also measured in order to assist in studying the dissolution reaction.

Sorenson (6) indicated that there was no effect of current density on the apparent valence. Actually, the current density is a vital factor affecting the apparent valence. This is in agreement with the report of Marsh and Schaschl (11), in which they suggested that removal of "chunks of iron" containing several atoms during anodic dissolution occurred only at a high current rate. In the case of zinc, the apparent valence approaches its normal oxidation state of two at low current densities (0.001 amp/cm^2). Since zero current would be the limiting value, the oxidation state of zinc could be zero if any zinc went into solution by local corrosion at open circuit. Thus the region between 0 and 0.001 amp/cm^2 must be one in which the apparent valence increases with current density. Above 0.001 amp/cm^2 , the valence decreases rapidly until a current density of 0.03 amp/cm^2 is reached and above which the apparent valence remains almost constant. This means that the apparent valence is proportional to the current density when it is less than 0.03 amp/cm^2 , above this value the apparent valence will remain constant (assuming the dissolution of zinc is the only reaction occurring).

The experimental data for the anodic dissolution of zinc in this investigation show that the apparent valence is a function of the concentration of nitrate solution, current density, and temperature. A plot of apparent valence against current density for various concentrations of nitrate ion shows similar behavior with each

concentration giving a different apparent valence. If the deviation of the valence from the normal valence, i.e., $V - V_i$, is associated with a rate process, then it might be expected to be proportional to $(C_{\text{NO}_3^-})^a (i)^b$, with the temperature dependence associated with the proportionality constant. This relationship is expressed mathematically

$$\text{as: } 2 - V_i = k(C_{\text{NO}_3^-})^a (i)^b$$

$$\text{or } V_i = 2 - k(C_{\text{NO}_3^-})^a (i)^b \quad (1)$$

Therefore, log-log plots of $2 - V_i$ versus $C_{\text{NO}_3^-}$ were prepared at constant current densities. Straight lines resulted and are shown in Figures 9 to 11. Their slopes, which determined the constant "a", were as follows:

$$t = 25^\circ\text{C}, \quad \text{slope}_{\text{ave}} = 0.378 \pm 0.04$$

$$t = 40^\circ\text{C}, \quad \text{slope}_{\text{ave}} = 0.372 \pm 0.05$$

$$t = 55^\circ\text{C}, \quad \text{slope}_{\text{ave}} = 0.362 \pm 0.06$$

$$a_{\text{ave}} = 0.371 \text{ (for temperatures from 25 to } 55^\circ\text{C)}$$

Similar plots were prepared for varying current densities at constant nitrate ion concentration. Straight lines were also obtained as shown in Figures 12 to 14, and their slopes, "b", were as follows:

$$t = 25^\circ\text{C}, \quad \text{slope}_{\text{ave}} = 0.622 \pm 0.10$$

$$t = 40^\circ\text{C}, \quad \text{slope}_{\text{ave}} = 0.628 \pm 0.10$$

$$t = 55^\circ\text{C}, \quad \text{slope}_{\text{ave}} = 0.613 \pm 0.08$$

$$b_{\text{ave}} = 0.624 \text{ (for temperatures from 25 to } 55^\circ\text{C)}$$

The slopes were the same within experimental error.

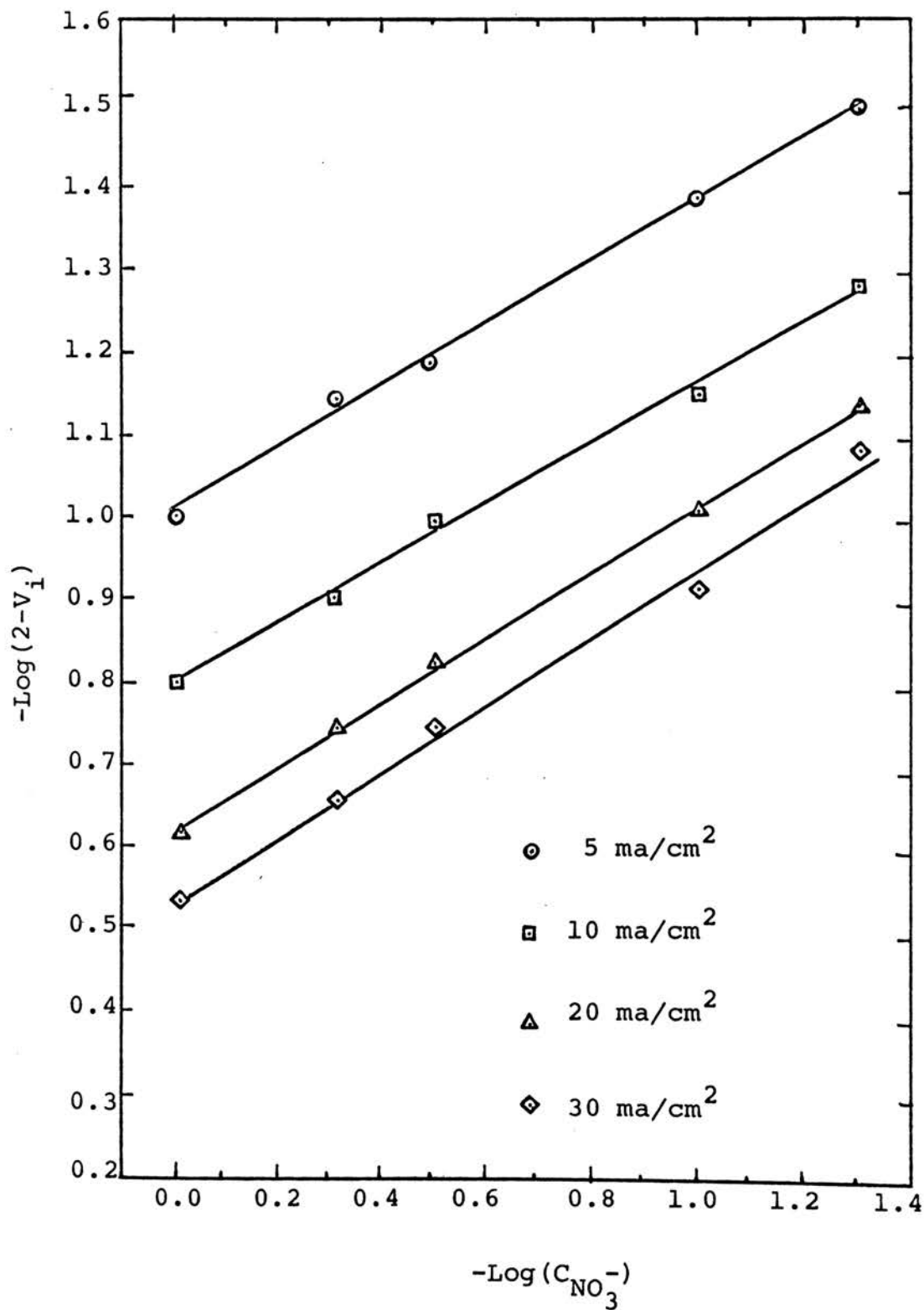


Figure 9. The effect of nitrate ion concentration on the apparent valence of zinc undergoing anodic dissolution at 25°C.

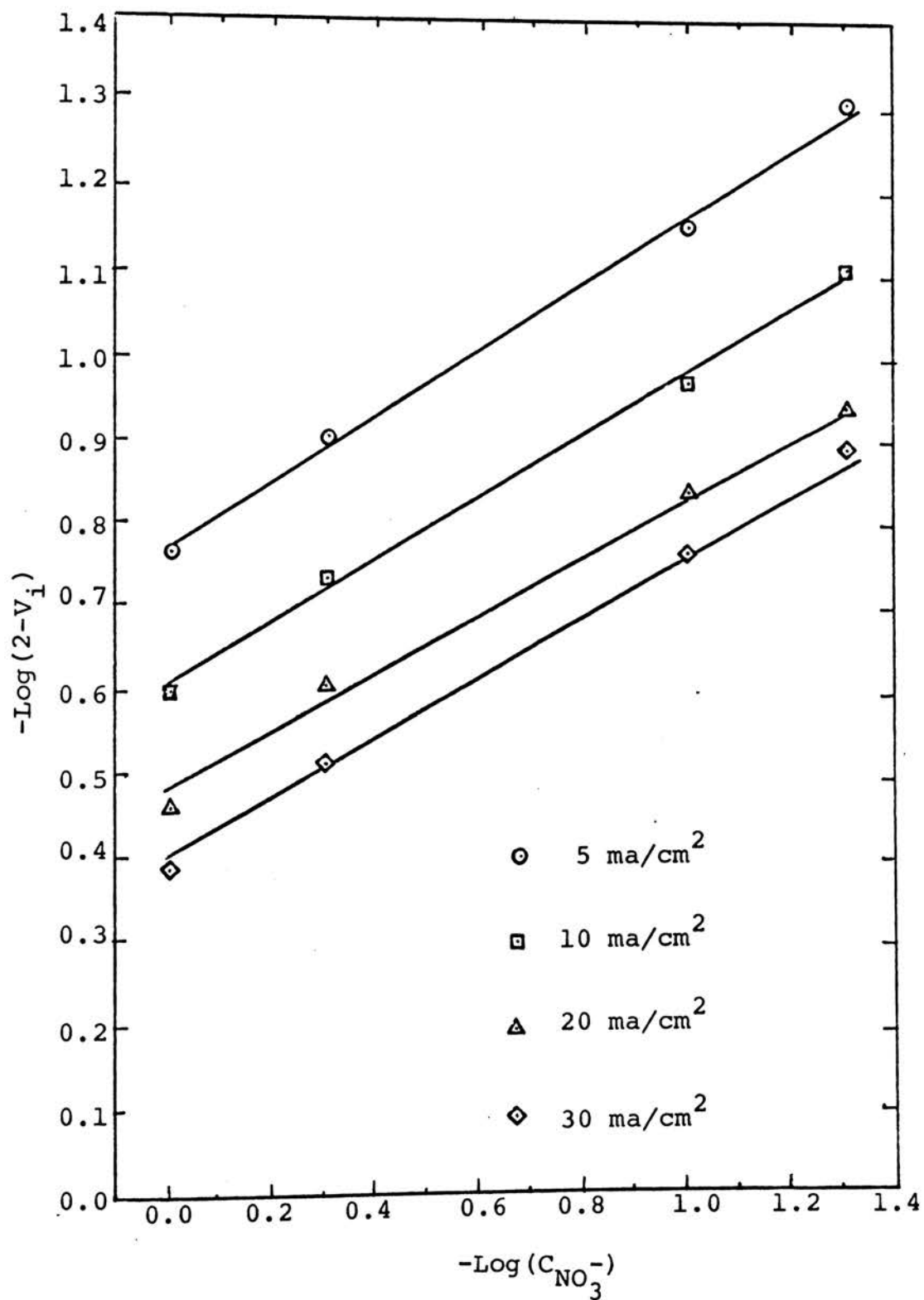


Figure 10. The effect of nitrate ion concentration on the apparent valence of zinc undergoing anodic dissolution at 40°C.

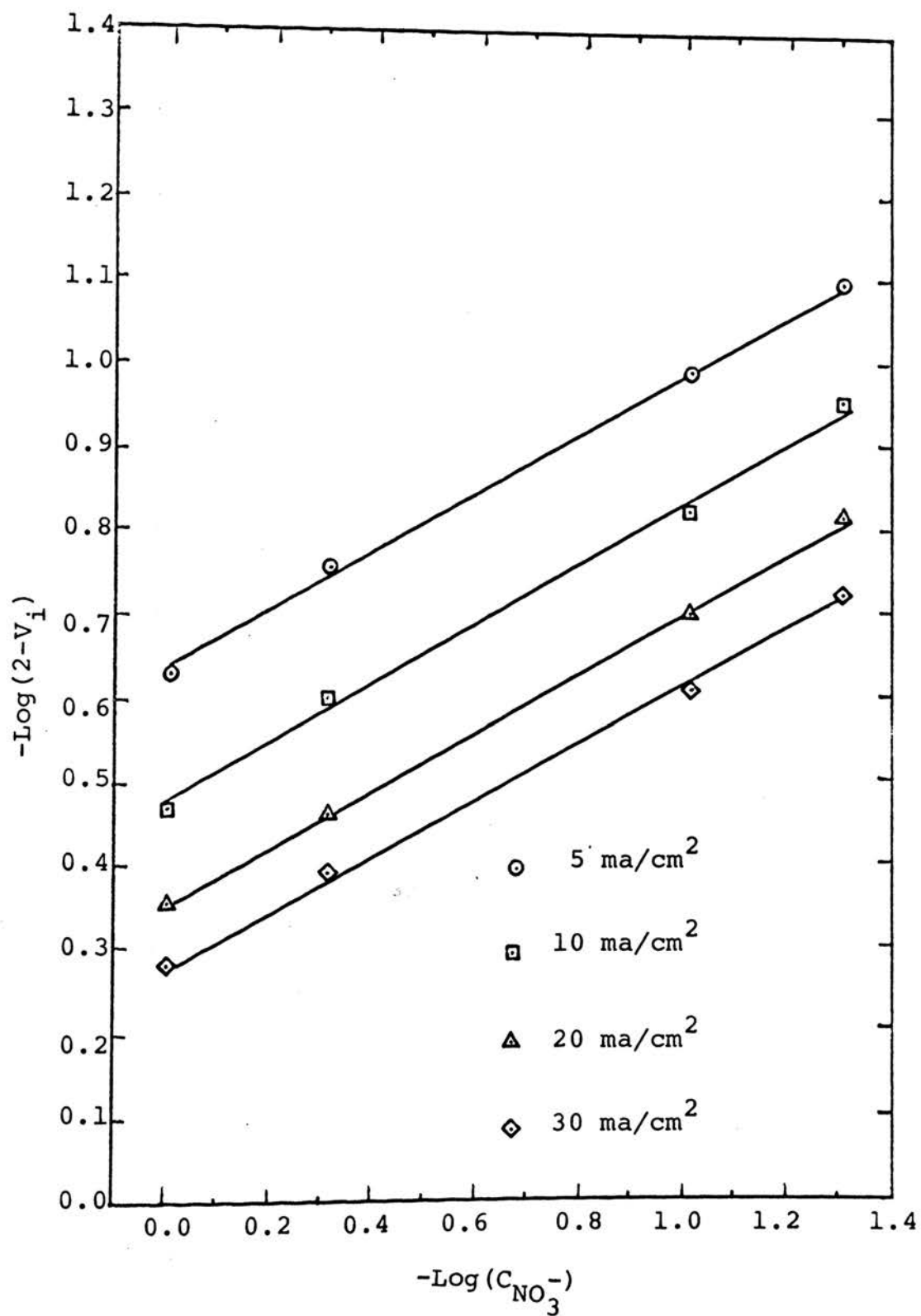


Figure 11. The effect of nitrate ion concentration on the apparent valence of zinc undergoing anodic dissolution at 55°C .

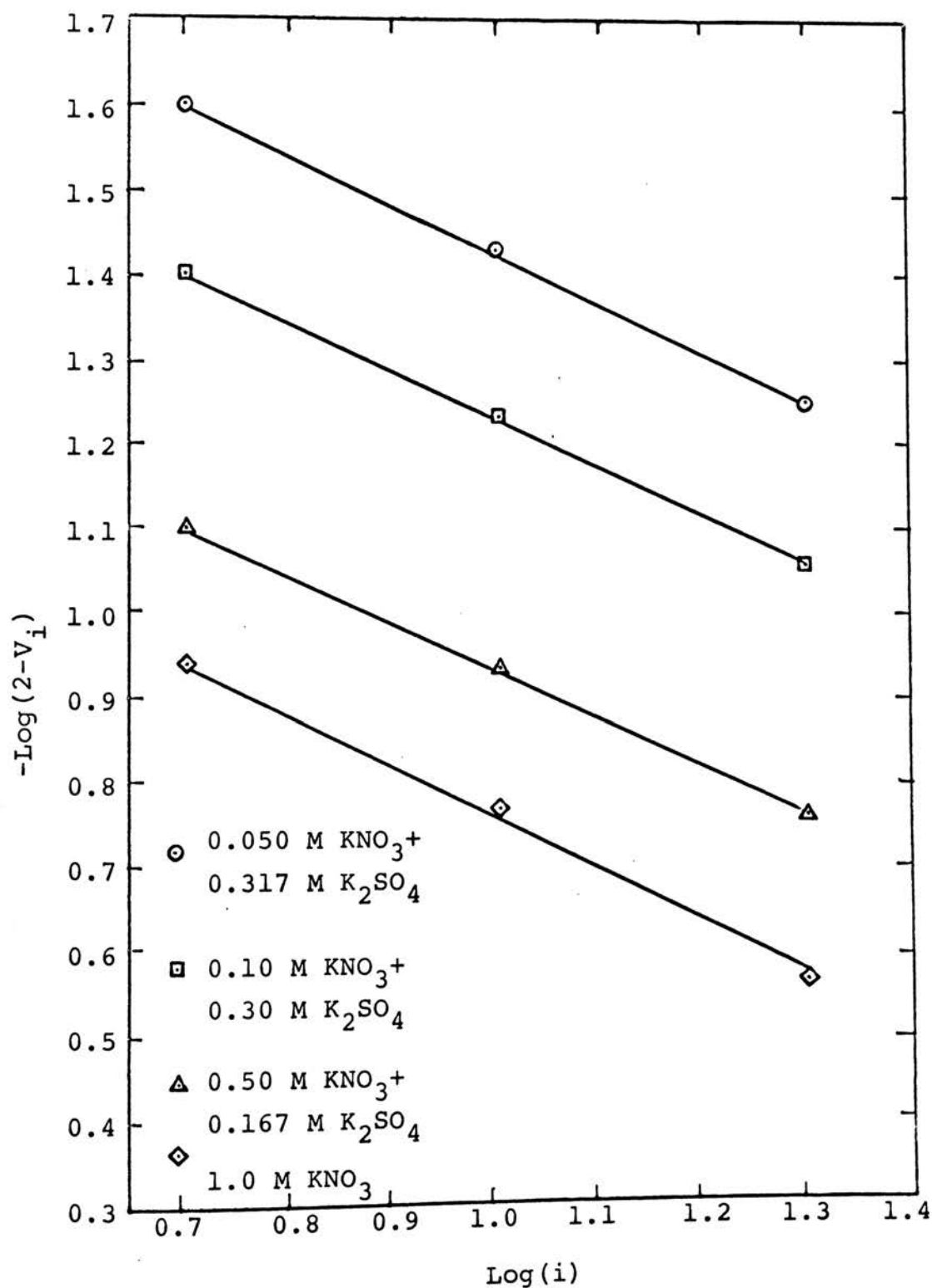


Figure 12. The effect of current density on the apparent valence of zinc undergoing anodic dissolution at 25°C.

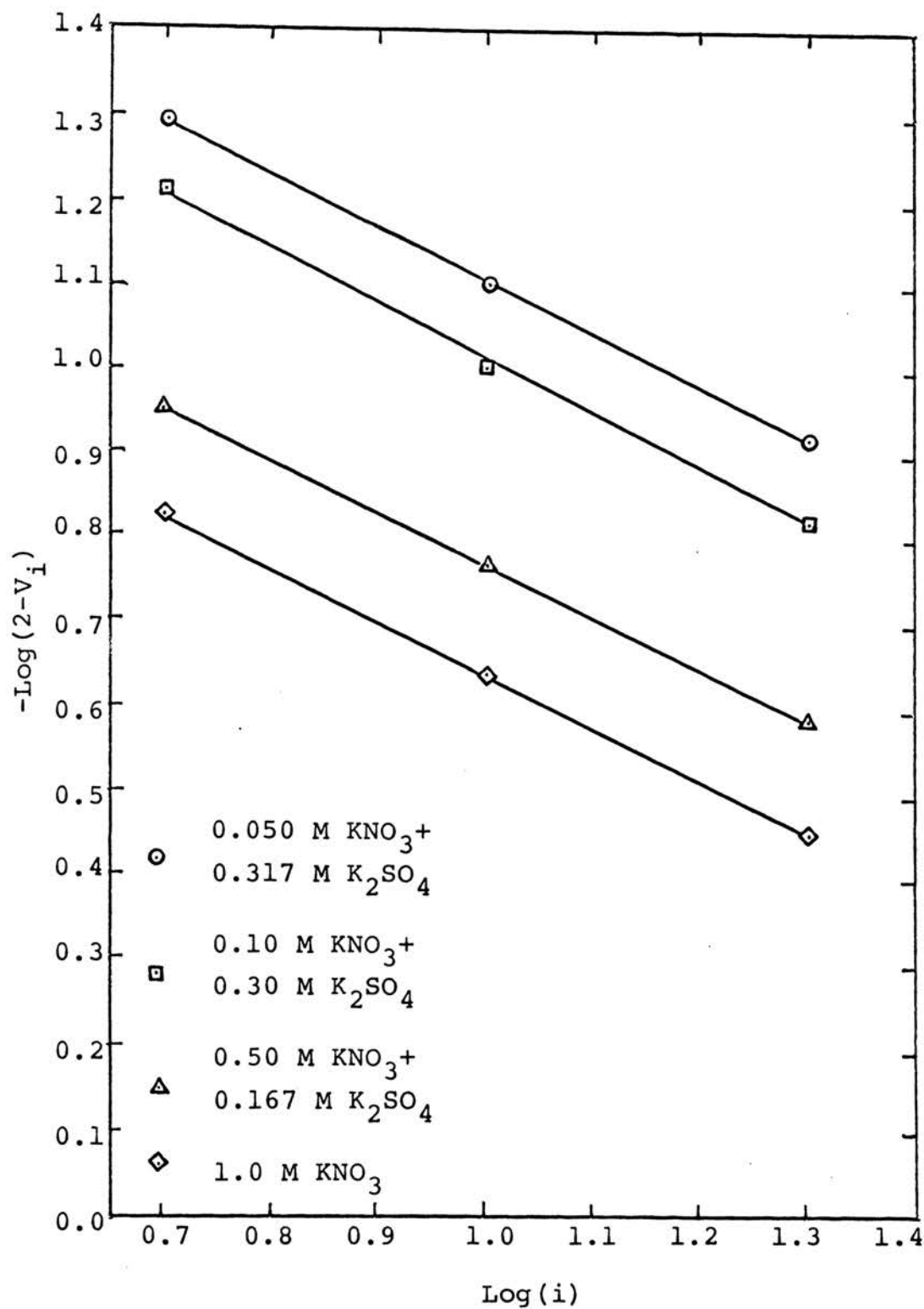


Figure 13. The effect of current density on the apparent valence of zinc undergoing anodic dissolution at 40°C.

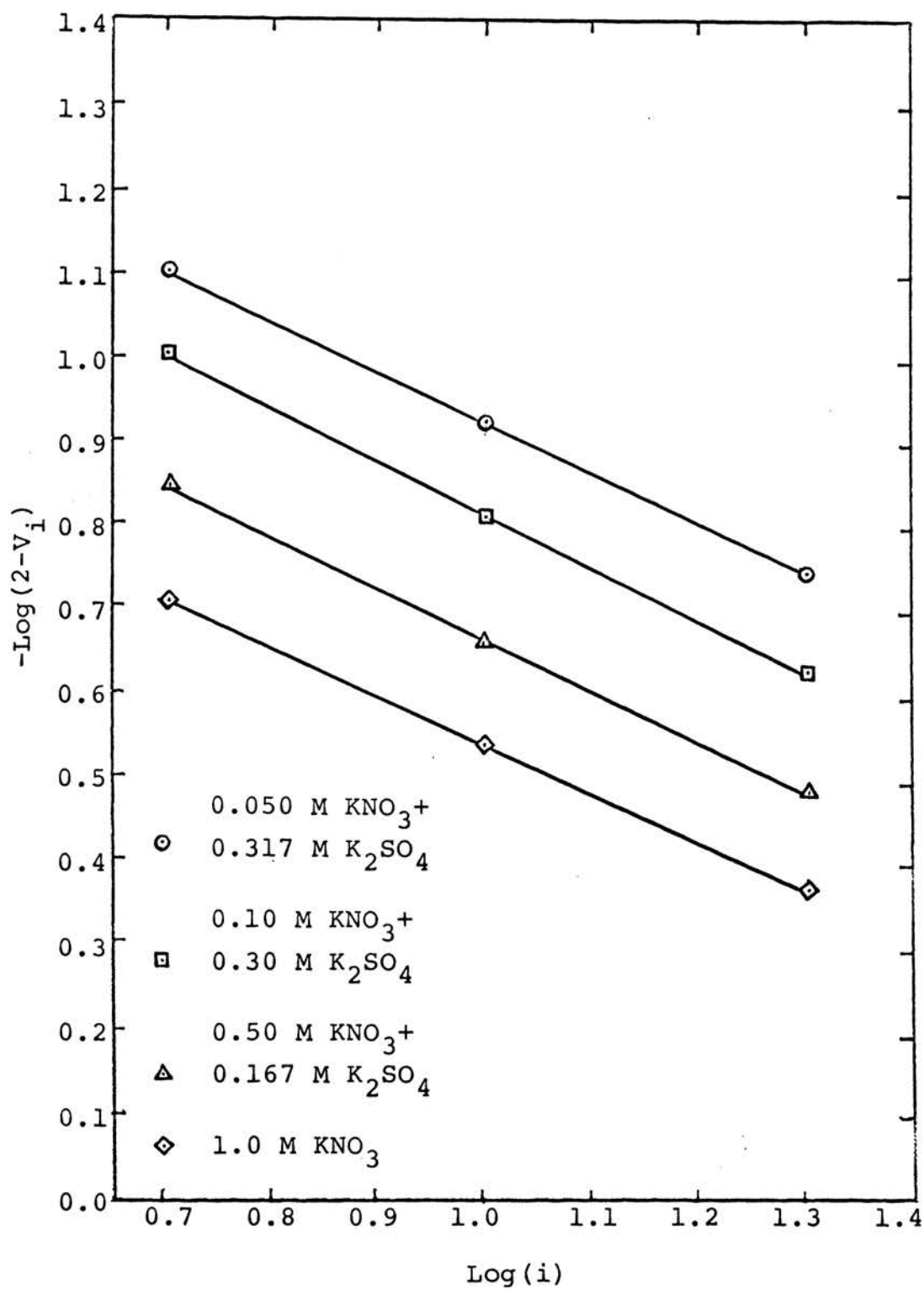


Figure 14. The effect of current density on the apparent valence of zinc undergoing anodic dissolution at 55°C .

Substituting these numerical values into equation (1):

$$V_i = 2 - k(C_{\text{NO}_3^-})^{0.371}(i)^{0.624} \quad (2)$$

Values for "k" can be calculated by substituting experimental data into equation (2) at 25°C: $V_i = 1.73$ when $C_{\text{NO}_3^-} = 1.0 \text{ M}$, and $i = 20 \text{ ma/cm}^2$. Substituting these values into equation (2):

$$1.73 = 2 - k_{(25)}(1.0)^{0.371}(20)^{0.624}$$

$$\therefore k_{(25)} = 0.042$$

At 40°C, $V_i = 1.67$ when $C_{\text{NO}_3^-} = 1.0 \text{ M}$, and $i = 20 \text{ ma/cm}^2$.

Substituting these values into equation (2), gives

$$k_{(40)} = 0.0513$$

At 55°C, $V_i = 1.61$ when $C_{\text{NO}_3^-} = 1.0 \text{ M}$, and $i = 20 \text{ ma/cm}^2$.

Substituting these values into equation (2), gives

$$k_{(55)} = 0.0606$$

A plot of $\log(k)$ versus $1/T$ was prepared. A straight line was obtained as shown in Figure 15, and its slope yielded an activation energy (E_a) of 2.3 kcal.

This relationship is in accord with the fact that the temperature coefficient would be expected to be relatively constant over the temperature range from 25 to 55°C.

The empirical equation of the apparent valence as a function of current density, nitrate ion concentration, and temperature is:

$$V_i = 2 - (C_{\text{NO}_3^-})^{0.371}(i)^{0.624}(2.09)\exp\left(\frac{-2,300}{RT}\right) \quad (3)$$

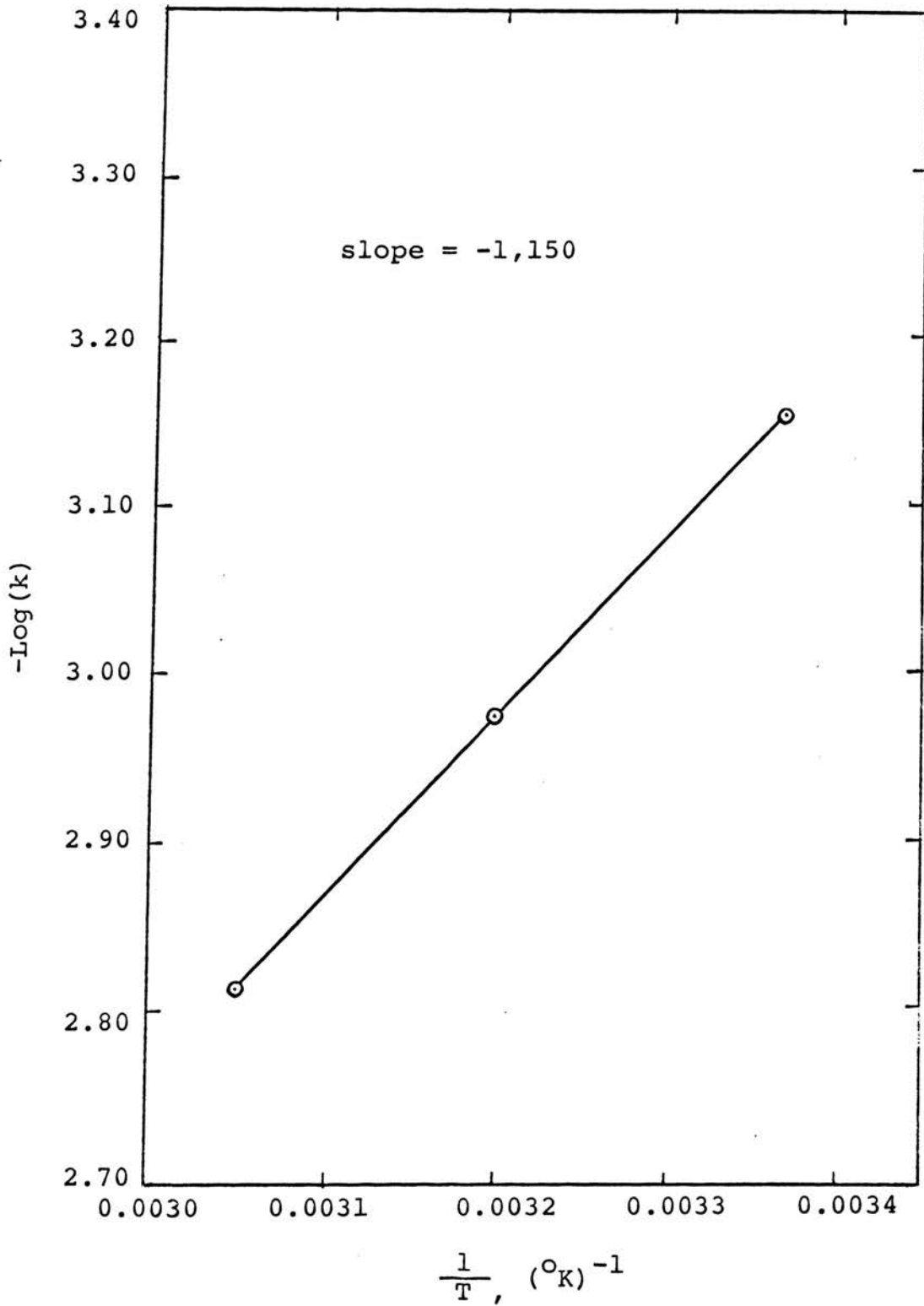


Figure 15. The effect of temperature on the apparent valence of zinc undergoing anodic dissolution.

Thus, the apparent valence can be predicted for any given concentration, current density (below approximately 30 ma/cm^2), and temperature within the range of this experiment.

For example:

1. When $C_{\text{NO}_3^-} = 0.30 \text{ M}$, $i = 10 \text{ ma/cm}^2$, and $t = 25^\circ\text{C}$

$$V_i \text{ (from experiment)} = 1.90$$

$$V_i \text{ (from equation 3)} = 1.89$$

2. When $C_{\text{NO}_3^-} = 0.050 \text{ M}$, $i = 20 \text{ ma/cm}^2$, and $t = 40^\circ\text{C}$

$$V_i \text{ (from experiment)} = 1.89$$

$$V_i \text{ (from equation 3)} = 1.89$$

3. When $C_{\text{NO}_3^-} = 1.0 \text{ M}$, $i = 15 \text{ ma/cm}^2$, and $t = 55^\circ\text{C}$

$$V_i \text{ (from experiment)} = 1.65$$

$$V_i \text{ (from equation 3)} = 1.67$$

Beyond approximately 30 ma/cm^2 , the apparent valence is constant. A modification of equation (2) can be written as:

$$V_i = 2 - k'(C_{\text{NO}_3^-})^{0.371} \quad (4)$$

Similarly, at 25°C , $V_i = 1.68$ when $C_{\text{NO}_3^-} = 1.0 \text{ M}$, and $i = 50 \text{ ma/cm}^2$. Substituting these values into equation (4), gives $k'_{(25)} = 0.32$

At 40°C , $V_i = 1.59$ when $C_{\text{NO}_3^-} = 1.0 \text{ M}$, and $i = 50 \text{ ma/cm}^2$.

This gives $k'_{(40)} = 0.41$

At 55°C , $V_i = 1.51$ when $C_{\text{NO}_3^-} = 1.0 \text{ M}$, and $i = 50 \text{ ma/cm}^2$.

This gives $k'_{(55)} = 0.49$

A plot of $\log(k')$ versus $1/T$ was prepared. A straight line was obtained as shown in Figure 16, and its slope yielded an activation energy (E_a) of 2.7 kcal.

This relationship is in accord with the fact that the temperature coefficient would be expected to be relatively constant over the temperature range from 25 to 55°C.

The empirical equation of the apparent valence as a function of current density, nitrate ion concentration, and temperature is:

$$V_i = 2 - (C_{\text{NO}_3^-})^{0.371} (32.3) \exp\left(\frac{-2,700}{RT}\right) \quad (5)$$

Thus, the apparent valence can be predicted for any given concentration, current density (beyond approximately 30 ma/cm²), and temperature within the range of this experiment.

For example:

1. When $C_{\text{NO}_3^-} = 0.50 \text{ M}$, $i = 100 \text{ ma/cm}^2$, and $t = 25^\circ\text{C}$

$$V_i \text{ (from experiment)} = 1.77$$

$$V_i \text{ (from equation 5)} = 1.76$$
2. When $C_{\text{NO}_3^-} = 0.10 \text{ M}$, $i = 50 \text{ ma/cm}^2$, and $t = 40^\circ\text{C}$

$$V_i \text{ (from experiment)} = 1.82$$

$$V_i \text{ (from equation 5)} = 1.83$$
3. When $C_{\text{NO}_3^-} = 1.0 \text{ M}$, $i = 40 \text{ ma/cm}^2$, and $t = 55^\circ\text{C}$

$$V_i \text{ (from experiment)} = 1.52$$

$$V_i \text{ (from equation 5)} = 1.51$$

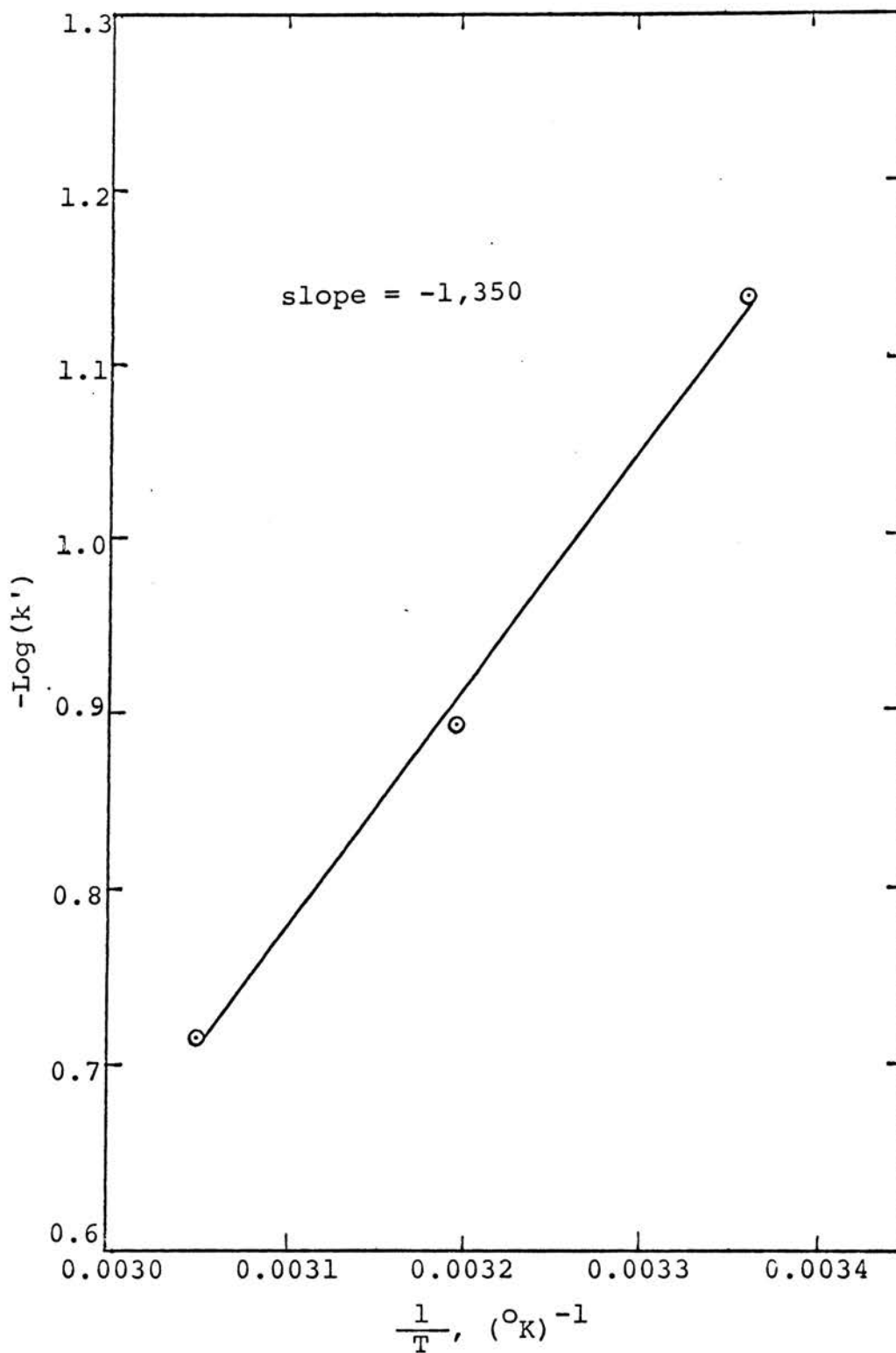


Figure 16. The effect of temperature on the apparent valence of zinc undergoing anodic dissolution.

Notation:

V_i = apparent valence

$C_{\text{NO}_3^-}$ = concentration of nitrate ion, gmols/liter

i = current density, ma/cm²

T = absolute temperature, °K

a = constant, independent of concentration of nitrate ion

b = constant, independent of current density

k, k' = constant, dependent on temperature

R = gas constant, cal °K⁻¹ gmol⁻¹

It appears that a likely mechanism is as follow:

The zinc anode is normally covered with protective film (oxide, hydroxide) prior to electrolysis. As an external current is applied, local elements, consisting of local cathodes (impurities, dislocations in the zinc structure, etc.) and local anodes are uncovered. These local elements allow corrosion to occur. Due to the high hydrogen overpotential on zinc, if corrosion is to proceed, the H⁰ formed on the local cathodes must be removed by oxidizing agents (NO₃⁻) in the electrolyte, i.e., nitrate ions serving as depolarizers. The hydrogen forming on the local cathodes protects these areas from corrosion, but allows metal in the surrounding area to be dissolved until the local cathode is detached. This gives rise to the metal particles in solution or the "disintegration" of the anode. Thus, it seems that the disintegration rate is proportional to the local corrosion rate and that these

phenomena are responsible for the observed deviation of anodic behavior from Faraday's law. This leads to an apparent valence which is less than normal. Experimentally, the apparent valence reaches a limiting value beyond current densities of approximately 30 ma/cm^2 . Below 30 ma/cm^2 , the apparent valence increases and approaches the normal valence as a limiting value. This result suggests that at low current densities, the local corrosion (and disintegration) rate is increasing exponentially with external current. This can be explained by the large ratio of protected area to local elements which causes the local elements to spread laterally. At high current densities, the local corrosion rate increases linearly with external current. This can be explained by the small ratio of protected area to local elements, thus, the local elements increase linearly with increasing current density.

The amalgamated zinc electrode (17), for which the faradaic and experimental equivalence agree, can be explained by the proposed mechanism. Mercury, which is cathodic to zinc has a very high hydrogen overpotential and the hydrogen evolution rate is controlled by the discharge of H^+ . Therefore, H^0 is sparingly formed on mercury and the depolarizer cannot accelerate local corrosion. Thus, an apparent valence of two is normally obtained, even in nitrate solutions.

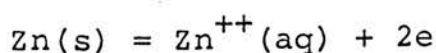
It is possible that disintegration might occur in any kind of electrolyte, as it is a function of current density,

temperature, and both the nature of the electrolyte and electrode. The disintegration rate is facilitated by the action of oxidizing agents, when corrosion is cathodically controlled by the combination of hydrogen atoms. Thus H^O is removed from the local cathodes continuously. The metallic particles from the anode are very active due to their tiny size and react rapidly with the electrolyte.

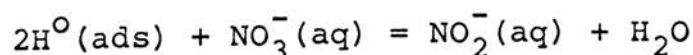
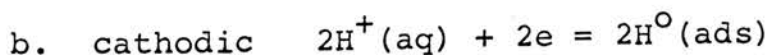
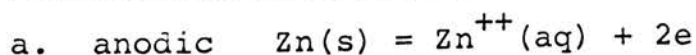
Several quantitative studies have been made to determine the amount of nitrite ion formed during electrolysis in potassium nitrate (17). Results confirmed that the amount of nitrite ion formed accounted for the difference between the amount of zinc dissolved based on a valence of plus two and the actual weight loss of the zinc electrode, assuming the nitrate ion to be an oxidizing agent. Thus, the metal particles were most probably consumed by corrosion made possible by the nitrate depolarizer.

Accordingly, the reactions involved in the dissolution process may be written:

Anodic reaction (reaction responsible for current in the external circuit)

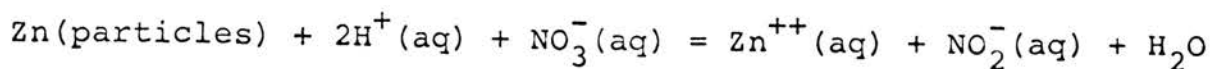


Local corrosion reaction



Disintegration reaction (particles removed by corrosion)

Zn(electrode) = Zn(particles)



On the basis of these reactions, a mathematical model for the anodic dissolution of zinc in nitrate ion can be derived as follows: (see page 54 for notation)

The total dissolution rate is the sum of the electrochemical, local corrosion, and disintegration rates,

$$r_T = r_E + r_L + r_D \quad (6)$$

The electrochemical dissolution rate is proportional to the current, therefore,

$$r_E = k_1(i) \quad (7)$$

The rate of local corrosion would be dependent on several variables. Among these are the electronegativity of the metal, the number of local cathodes (impurity and metallic structure) and the rate at which they are uncovered (external current), the concentration of hydrogen ions, and the concentration of the depolarizer (NO_3^-). For a given metal and electrolyte of constant pH, the local corrosion rate is:

$$r_L = k_2 (C_{\text{NO}_3^-})^m (i)^n \quad (8)$$

Since disintegration results directly from corrosion, a first approximation would be to assume that the disintegration rate is directly proportional to it, i.e.,

$$r_D = k'_3 (r_L) = k_3 (C_{\text{NO}_3^-})^m (i)^n \quad (9)$$

$$\begin{aligned}
 r_T &= k_1(i) + k_2(C_{\text{NO}_3^-})^m(i)^n + k_3(C_{\text{NO}_3^-})^m(i)^n \\
 &= k_1(i) + k_4(C_{\text{NO}_3^-})^m(i)^n \quad (10)
 \end{aligned}$$

$$\begin{aligned}
 \text{But, } V_i &= \frac{r_E}{r_T}(2) \\
 &= \frac{2k_1(i)}{k_1(i) + k_4(C_{\text{NO}_3^-})^m(i)^n} \\
 &= \frac{2}{1 + k'(C_{\text{NO}_3^-})^m(i)^{n'}} \\
 &= 2[1 - k'(C_{\text{NO}_3^-})^m(i)^{n'} + \dots - \dots] \quad (11)
 \end{aligned}$$

Since $k'(C_{\text{NO}_3^-})^m(i)^{n'} \ll 1$, then the higher terms of equation (11) may be omitted and

$$\begin{aligned}
 V_i &= 2[1 - k'(C_{\text{NO}_3^-})^m(i)^{n'}] \\
 &= 2 - k(C_{\text{NO}_3^-})^m(i)^{n'}
 \end{aligned}$$

$$\text{or, } 2 - V_i = k(C_{\text{NO}_3^-})^m(i)^{n'} \quad (12)$$

The theoretical equation (12), based on the proposed mechanism and hypothesis, has the same form as the empirical equation (1), derived from experimental data.

Notation:

r_T = total rate of anodic dissolution (experimental)

r_E = rate of anodic dissolution from Faraday's law

r_L = rate of anodic dissolution by local corrosion

r_D = rate of anodic dissolution by disintegration

i = current density

$C_{NO_3^-}$ = concentration of nitrate ion

V_i = apparent valence

$k_1, k_2, k_3', k_3, k_4, k',$ and k = constants, dependent on
temperature

m = constant, independent of concentration of nitrate ion

n and n' = constants, independent of current density

This concept of the deviation of the anodic dissolution of zinc from Faraday's law can be readily extended to other metals. For instance, magnesium is found to disintegrate in almost all aqueous solutions. As hydrogen can be readily seen evolving from its surface, it apparently is reactive enough or has a low hydrogen overpotential so that local corrosion (and disintegration) can occur without a depolarizer.

Cadmium fits in the same category as zinc. During anodic dissolution, no hydrogen is observed on its surface so that a depolarizer is necessary if it is to exhibit an "uncommon valence".

Other studies with magnesium (36) have indicated both anion and cation effects on the apparent valence. For zinc, essentially no effect was found for sulfate solutions containing Cl^- , Br^- , I^- , and $C_2H_3O_2^-$ ions. Since none of these ions could act as oxidizers, they would not promote

local corrosion so that differences in the solubilities of their metallic salts or anion adsorption characteristics could be noted.

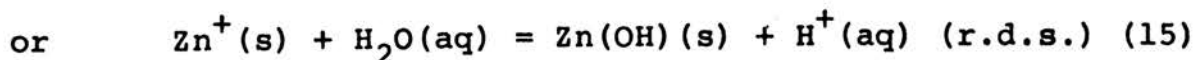
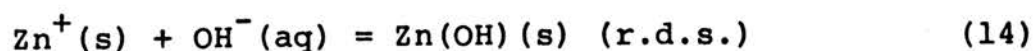
The addition of zinc cations also had no effect in contrast to the behavior of magnesium. The magnesium ions have a definite effect on the potential of the local anodes, thus affecting the overpotential of the local corrosion reaction which ultimately yields hydrogen. For zinc, the local corrosion rate is controlled by the NO_3^- depolarizer, thus there is no cation effect.

From the anodic potential-current density plots, a linear relationship for the Tafel curve below current densities of 10 ma/cm^2 was observed (Figures 7 and 8). A summary of Tafel curve slopes is listed as follows:

Electrolyte	Tafel curve slope (volts)		
	25°C	40°C	55°C
0.050 M KNO_3 +0.317 M K_2SO_4	0.080	0.060	0.065
0.10 M KNO_3 +0.30 M K_2SO_4	0.070	0.070	0.055
0.50 M KNO_3 +0.167 M K_2SO_4	0.080	0.065	0.060
1.0 M KNO_3	0.085	0.090	0.070
0.010 M ZnBr_2 +0.320 M K_2SO_4	0.040	0.025	0.020
0.10 M ZnBr_2 +0.230 M K_2SO_4	0.020	0.015	0.020
0.010 M ZnCl_2 +0.320 M K_2SO_4	0.020	0.020	0.015
0.10 M ZnCl_2 +0.230 M K_2SO_4	0.025	0.020	0.015
0.010 M ZnSO_4 +0.320 M K_2SO_4	0.025	0.020	0.020
0.10 M ZnSO_4 +0.20 M K_2SO_4	0.020	0.015	0.020

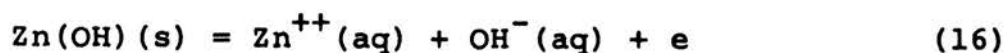
Electrolyte	Tafel curve slope (volts)		
	25°C	40°C	55°C
0.010 M ZnI ₂ +0.320 M K ₂ SO ₄	0.025	0.020	0.020
0.10 M ZnI ₂ +0.230 M K ₂ SO ₄	0.015	0.015	0.020
0.010 M Zn(C ₂ H ₃ O ₂) ₂ +0.320 M K ₂ SO ₄	0.030	0.020	0.025
0.10 M Zn(C ₂ H ₃ O ₂) ₂ +0.230 M K ₂ SO ₄	0.020	0.015	0.015
0.010 M Zn(NO ₃) ₂ +0.320 M K ₂ SO ₄	0.025	0.035	0.045
0.10 M Zn(NO ₃) ₂ +0.230 M K ₂ SO ₄	0.055	0.060	0.065

Calculation of i_0 , i.e., the exchange current, revealed a magnitude of ca. 10^{-6} for K₂SO₄-KNO₃ solutions and 10^{-3} for zinc salt solutions. From these values, the rate can be inferred to be activation controlled. It can be seen from the table that all slopes in K₂SO₄-KNO₃ solutions fall in the range of values 0.055 to 0.090 volts. This is closest to a theoretical slope of $2.3RT/F$ which indicates that the rate determining step is a non-charge transfer step following the first charge transfer. Since no apparent concentration dependence can be seen, the species involved in this process might be either OH⁻ or H₂O. The mechanism could be as follows:



It can also be seen from the table that all slopes in zinc salt solutions fall in the range of values 0.015 to 0.065

volts, with the majority being between 0.015 to 0.025 volts. This is closest to a theoretical slope of $2.3(2RT/3F)$ which indicates a rate determining step as the second charge transfer. A possible reaction is,



Reaction (16) shows the dependence on zinc ions in solution. With an appreciable concentration, the reverse rate of reaction (16) would be increased, thus decreasing its net rate. If reaction (16) is slowed to such an extent that it becomes slower than reaction (14) or (15) (in $\text{K}_2\text{SO}_4\text{-KNO}_3$ solutions), then the rate determining step will become reaction (16) in zinc salt solutions.

Apparently the film formed on the anode during electrolysis in solutions containing nitrate ions is protective to the metal (as differentiated from its role as a depolarizer at the local cathodes). This would add an ohmic drop to the potential, resulting in the higher observed values.

CHAPTER V

RECOMMENDATIONS

Further studies of anodic dissolution of zinc in salt solutions, such as KBr, KI, etc., by EDTA titration and measurement of electrode weight losses would allow an accurate check of the results reported herein.

Using different grades of zinc with respect to impurities for the anode (especially some low hydrogen overpotential metal as an impurity) may help in correlating the deviation from Faraday's law with the amount of active impurities in the anode.

High anodic current studies (up to one amp/cm²) and low current studies (below 0.5 ma/cm²) would provide a more inclusive picture of the current density and apparent valence relationship.

A micro-analysis of the anolyte to determine if hydrogen is evolved from the zinc anode during electrolysis might be helpful in confirming the mechanism proposed in this investigation. A measurement of dissolution rates at various pH's might also help in the confirmation.

CHAPTER VI

LIMITATIONS

Temperature. When the thermoregulator was set at a certain temperature, the reacting solution was assumed to remain at the same temperature. However, the temperature of the electrolyte deviated $\pm 2^{\circ}\text{C}$ because of the poor conduction of the glass cell.

EDTA Titration. Two to three ml of EDTA solution was usually used in each titration. Thus, even using a micro-burette, an error of one drop in titration could introduce a relative error of one to three percent.

Weighing. The drying and weighing method was described as being repeated until a constant weight was obtained. However, in the actual case, constant weight was assumed to be reached when the difference between the last and the previous weight was less than 0.0008 gram.

Purity of Zinc. Zinc metal of 99.99+ percent purity was used in this investigation. The impurities are reported as follows: Mg < 1 ppm, Pb < 7 ppm, Si < 1 ppm, Cu < 3 ppm, Cd < 1 ppm, and Ag < 5 ppm. These data are from a spectrographic analysis.

CHAPTER VII

SUMMARY AND CONCLUSIONS

The purpose of the present studies was to determine the effect of various neutral electrolytes, anodic current density, and temperature on the anodic dissolution of zinc. From the experimental data, a mechanism was obtained in accord with the results.

Most of the runs were accomplished using current densities of 1 to 50 ma/cm², in an electrolyte of unit ionic strength. The temperature was controlled by means of a constant temperature water bath, varying from 25 to 55°C. A titration with Disodium Ethylenediaminetetraacetate or a weighing method was used to determine the zinc dissolved during each run. The relationship of anodic current density to potential was also determined. The following results were obtained:

1. In K₂SO₄ solutions containing ZnSO₄, Zn(C₂H₃O₂)₂, ZnCl₂, ZnBr₂, or ZnI₂, zinc exhibits a normal valence of two within an experimental error of ±0.03. In K₂SO₄-ZnBr₂ solution, zinc shows the greatest deviation from normal valence.
2. In nitrate solutions, an apparent valence of less than two occurs, decreasing with increasing concentration of nitrate ion and temperature. The valence is also a function of the anodic current density.

The following empirical equation was derived which relates apparent valence to temperature, concentration of nitrate ion, and current density.

$$V_i = 2 - (C_{\text{NO}_3^-})^{0.371} (i)^{0.624} (2.09) \exp\left(\frac{-2,300}{RT}\right)$$

(for current densities below approximately 30 ma/cm²)

$$V_i = 2 - (C_{\text{NO}_3^-})^{0.371} (32.3) \exp\left(\frac{-2,700}{RT}\right)$$

(for current densities above approximately 30 ma/cm²)

3. Tafel plots show a linear relationship below a current density of 10 ma/cm²; the slope varies from 0.055 to 0.090 volts in KNO₃-K₂SO₄ solutions and 0.015 to 0.025 volts in zinc salt solutions.

It is concluded that the normal valence of zinc ions does not change during anodic dissolution. The apparent valence of less than two in nitrate solution arises in part or in whole as consequence of disintegration of the metal anode. The amount of disintegration is a function of current density, temperature, and the nature of the electrolyte. In nitrate solution, the disintegration rate is facilitated by the action of oxidizing agents, when local corrosion is cathodically controlled by the combination of hydrogen atoms.

BIBLIOGRAPHY

1. Bredig, G.: Anorganische Fermente, Leipzig (1901).
2. Burton, E.F.: Phil. Mag., 11, 425 (1906).
3. White, G.R.: J. Phys. Chem., 15, 723 (1911).
4. Del Boca, M.C.: "Electrolysis of Certain Salts of Metals in Liquid Ammonia", Helv. Chim. Acta., 16, 565 (1933).
5. Epelboin, I.: "Contribution a l'etude des Phenomenes Anodiques au Cours de la Dissolution Electrolytique des Metaux", Z. Elektrochem., 59, 689 (1955).
6. Sorensen, D.T., Davidson, A.W., and Kleinberg, J.: "The Anodic Oxidation of Zinc and Cadmium in Aqueous Solutions", J. Inorg. Nucl. Chem., 13, 64 (1960).
7. Petty, R.L., Davidson, A.W., and Kleinberg, J.: "The Anodic Oxidation of Magnesium Metal", J. Amer. Chem. Soc., 76, 364 (1954).
8. Raijola, E., and Davidson, A.W.: "The Anodic Oxidation of Magnesium Metal", J. Amer. Chem. Soc., 78, 556 (1956).
9. Laughlin, B.D., Kleinberg, J., and Davidson, A.W.: "Unipositive Beryllium as a Product of Anodic Oxidation", J. Amer. Chem. Soc., 78, 559 (1956).
10. Hoey, G.R., and Cohen, M.: "Corrosion of Anodically and Cathodically Polarized Magnesium in Aqueous Media", J. Electrochem. Soc., 105, 245 (1958).

11. Marsh, G.A., and Schaschl, E.: "The Difference Effect and Chunk Effect", J. Electrochem. Soc., 107, 960 (1960).
12. Robinson, J.L., and King, P.F.: "Electrochemical Behavior of Magnesium Anode", J. Electrochem. Soc., 108, 36 (1961).
13. Greenblatt, J.H.: "Gases Evolved at Magnesium Anodes and Cathodes in Neutral Salt Solution". Corrosion, 18, 1251 (1962).
14. Straumanis, M.E. and Mathis, D.L.: "The Disintegration of Beryllium During Its Dissolution in Hydrochloric Acid", J. Less-common Metals, 4, 213 (1962).
15. Straumanis, M.E. and Bhatia, B.K.: "Disintegration of Magnesium While Dissolving Anodically in Neutral and Acidic Solutions", J. Electrochem. Soc., 110, 359 (1963).
16. Evans, U.R.: "Corrosion and Oxidation of Metals", 883, Edward Arnold, London (1960).
17. Stoner, G.E.: "The Anodic Dissolution of Zinc in Aqueous Solution", M.S. Thesis, University of Missouri at Rolla (1963).
18. Wang, Y.: "Microscopic Observation on Etched Surfaces of Zinc Single Crystals and on Anodic Dissolution", M.S. Thesis, University of Missouri at Rolla (1964).
19. Daniels, W.J.: "The Dissolution of Deformed Magnesium in Sulfuric Acid", M.S. Thesis, University of Missouri at Rolla (1964).

20. Thiel, A., and Eckell, J.: Korrosion u. Metallachutz, 4, 121 (1928), 4, 145 (1928).
21. Straumanis, M.E., and Wang, N.Y.: "The Difference Effect on Aluminum Dissolving in Hydrofluoric and Hydrochloric Acids", J. Electrochem. Soc., 102, 304 (1955).
22. Straumanis, M.E. and Chen, P.C.: "The Difference Effect on Titanium Dissolving in Hydrofluoric Acid", J. Electrochem. Soc., 98, 351 (1951).
23. James, W.J., Straumanis, M.E., Bhatia, B.K., and Johnson, J.W.: "The Difference Effect on Magnesium Dissolving in Acids", J. Electrochem. Soc., 109, (1962).
24. Kirkov, P.: "Influence of Solvent Composition on Electrode Potential", Glasnik Hem., Drustva, Beograd, 299-305 (1961).
25. James, W.J., and Stoner, G.E.: "Valence Exhibited by Zinc Amalgam Anodically Dissolving in Nitrate Solutions", J. Amer. Chem. Soc., 85, 1354 (1963).
26. Sun, Y.C.: "The Anodic Dissolution of Cadmium in Aqueous Solution", M.S. Thesis, University of Missouri at Rolla, (1964).
27. Hoar, T.P.: Private Communication to W.J. James, (1962).
28. Kochman, E.D., and Vozdvizhenskii, G.S.: "Voltamperometric Study of Anodic Polarization of Zinc in Aqueous Solution", Anodnaya Zashchita Metal. Kazansk Awiats. Inst., 360-375 (1964).

29. Yoshino, Hisao: "Anode Performance of Zinc in Fresh Water at Elevated Temperature", Tokyo Kogyo Shikenaho Hokoku, 57, 551 (1962).
30. Krochmal, F., and Beltowsha, M.: "Influence of Cations on Anodic Behavior of Zinc", Zeszyty Nauk, Uniw., Poznanic, Mat. Fiz. Chem., 61 (1963).
31. Krochmal, F., and Stencel, M.: "Influence of Anions on Anodic Behavior of Zinc", Zeszyty Nauk, Uniw., Poznanic, Mat. Fiz. Chem., 34 (1962).
32. Krochmal, F.: "Influence of Some Anions on Anodic Behavior of Zinc in KCl Solution", Zeszyty Nauk, Uniw., Poznanic, Mat. Fiz. Chem., 47 (1964).
33. Flerov, V.N.: "Variation of the Electrochemical Characteristics of Certain Powdered Electrodes After a prolonged Inaction", Izv. Vysshikh Utchebn. Zaveden, Khim Tekhnol, 449 (1963).
34. Uhlig, H.H., and Krutenat, R.: "Formation of Dissolved Atomic Hydrogen by Electrochemical Polarization", J. Electrochem. Soc., 111, 1303 (1964).
35. Chang, C.P., Li, C.C., and Shieh, S.T.: "Electrochemical Mechanism of Anodic Dissolution and Self-dissolution of Zinc in Potassium Hydroxide Solution", (University of Fudan, China) Hua Hsueh Hsueh Pao, 29, 236 (1963).
36. Chi, C.K.: "The Dissolution of Magnesium in Strong Acids and Neutral Solutions", M.S. Thesis, University of Missouri at Rolla, (1965).

APPENDIX

APPENDIX A

MATERIALS

The following is a list of the major chemicals used in this investigation.

1. Disodium Ethylenediaminetetraacetate. ACS reagent grade, Fisher Scientific Co., Fair Lawn, N.J.
2. Triethanolamine, N.F. Reagent grade, Fisher Scientific Co., Fair Lawn, N.J.
3. Potassium Chloride. ACS reagent grade, Fisher Scientific Co., Fair Lawn, N.J.
4. Potassium Nitrate. ACS reagent grade, Fisher Scientific Co., Fair Lawn, N.J.
5. Potassium Bromide. ACS reagent grade, Fisher Scientific Co., Fair Lawn, N.J.
6. Potassium Acetate. ACS reagent grade, Fisher Scientific Co., Fair Lawn, N.J.
7. Potassium Iodide. ACS reagent grade, Fisher Scientific Co., Fair Lawn, N.J.
8. Potassium Sulfate. ACS reagent grade, Fisher Scientific Co., Fair Lawn, N.J.
9. Zinc Acetate. Reagent grade, Fisher Scientific Co., Fair Lawn, N.J.
10. Zinc Bromide. Reagent grade, Fisher Scientific Co., Fair Lawn, N.J.
11. Zinc Chloride. ACS reagent grade, Fisher Scientific Co., Fair Lawn, N.J.

12. Zinc Iodide. Reagent grade, Fisher Scientific Co., Fair Lawn, N.J.
13. Zinc Nitrate. Reagent grade, Fisher Scientific Co., Fair Lawn, N.J.
14. Zinc Sulfate. ACS reagent grade, Fisher Scientific Co., Fair Lawn, N.J.
15. Hydrochloric Acid. ACS reagent grade, Fisher Scientific Co., Fair Lawn, N.J.
16. Zinc. 99.99+ percent purity, obtained by Dr. M.E. Straumanis from American Smelting and Refining Co., South Plainfield, N.J.

APPENDIX B

APPARATUS

Constant Temperature Bath Apparatus

1. Water Bath. Fisher Scientific Co., Pittsburg, Pa.
2. Heater. 110 v, ac, Fisher Scientific Co.,
Pittsburg, Pa.
3. Motor, Stirrer. Type v-10, 115 v, Palo Laboratory
Supplies, N.Y.
4. Electronic Relay. Type Cenco, 115 v, ac, Central
Scientific Co., Chicago, Ill.
5. Thermo-regulator. Type CRC, The Chemical Rubber
Co., Cleveland, Ohio.

Electrolysis Apparatus

1. Milliammeter. Model 931, Weston Electric Instrument
Corp., Newark, N.J.
2. Power Supply. 150 v, dc, Sangamo Co.
3. Resistance Box. Decade type, Graduated from 0 to
999,999 ohm in one ohm divisions, Clarostat Mfg. Co., Inc.,
Dover, N.H.
4. Recorder. Type VOM-5, Bausch-Lomb Co., Rochester,
N.Y.
5. Electrometer. Type 610B, Keithley Instruments Co.,
Cleveland, Ohio.
6. Timer. 120 v, Lab-Line Instruments, Inc.,
Melrose Park, Ill.

Miscellaneous Equipment

1. Semi-micro Balance. Model 2403, 120 v, Sartorius-werke AG., Gottingen, Germany.
2. pH Meter. Model 19, 115 v, Fisher Scientific Co., Pittsburg, Pa.
3. Nitrogen Tank Regulator. Kim Products, Inc., Burgin, Ky.
4. Hot Air Blower. 110 v, Racine Universal Motor Co., Racine, Wis.
5. Micro-burette. Shelback, 10 ml, 0.05 ml graduations, Fisher Scientific Co., Pittsburg, Pa.
6. Hand Grinder. Two-stage with grit number 64 and 600.

APPENDIX C

MISCELLANEOUS EXPERIMENTAL PROCEDURES

Standardization of Disodium EDTA Solution

The procedure for this part of the experimentation follows as a step-by-step operation.

1. Accurately weigh out approximately three-tenths of a gram of zinc metal of 99.99+ percent purity.
2. Transfer to a 100 ml volumetric flask and dissolve in 1:3 diluted HCl, mix thoroughly.
3. Withdraw 10 ml aliquot with a pipette.
4. Dilute to 100 ml with distilled water and heat to about 80°C.
5. Add 10 ml pH 10 buffer solution.
6. Add one drop of Erichrome Black-T indicator solution.
7. Titrate with 0.05 M Disodium EDTA solution (micro-burette) until one drop turns solution from reddish to blue.
8. Determine the zinc equivalent of the Disodium EDTA solution in gram zinc/ml of EDTA solution.

Treatment of White Precipitate and Gray Film on the Zinc Electrode

The following procedure was used for treating the gray film formed during the anodic dissolution of zinc in aqueous potassium nitrate solution.

1. One drop of 1:10 diluted HCl is put on the gray film of the metal electrode after an electrolysis.

2. The film surface is massaged with a rubber policeman.
3. Metal electrode is dipped into the original electrolyte for about 10 seconds.
4. Repeat the same procedure as before until the film completely flaked off the electrode into the original electrolyte.
5. Five ml of 1:1 diluted HCl solution is added to the electrolyte in order to dissolve the white precipitate.
6. The electrolyte is carefully transferred to a 250 ml volumetric flask and diluted.
7. The electrolyte is now ready for EDTA titration.

EDTA Titration of Electrolyte

1. Withdraw 25 ml aliquot with a pipette from the electrolyte.
2. The rest of the procedure is the same as described in the standardization of EDTA solution.

Preparation of Buffer Solution of PH 10

1. Weigh out 67.5 gram of NH_4Cl and transfer to a 1000 ml beaker.
2. Add 550 ml of concentrated NH_4OH to the beaker.
3. Dilute with distilled water to one liter in a volumetric flask.

Surface Preparation of Zinc Specimens

1. Remove all pits and etched placed from the metal surface on a water-flushed, two-stage hand grinder

equipped with grit numbers 64 and 600 abrasive cloth, proceeding from the coarse to the fine.

2. Examine the polished surface by eye until the surface appears perfectly flat, then wash with distilled water.
3. Preetch the electrode in 1:10 diluted H_2SO_4 for about 10 seconds.
4. Rinse the electrode with distilled water.

APPENDIX D
Experimental Data

TABLE I

APPARENT VALENCE OF ZINC DISSOLVING ANODICALLY IN 0.30 M
 K_2SO_4 SOLUTION AT 25°C

Time (sec)	Current* (ma)	Wt. of Zinc		Apparent Valence
		Calcd. (g)	Expt. (g)	
13,600	5	0.0230	0.0229	2.01
1,400	60	0.0285	0.0288	1.98

TABLE II

APPARENT VALENCE OF ZINC DISSOLVING ANODICALLY IN 0.050 M
 KNO_3 + 0.317 M K_2SO_4 SOLUTION AT 25°C

Time (sec)	Current* (ma)	Wt. of Zinc		Apparent Valence
		Calcd. (g)	Expt. (g)	
57,600	1	0.0195	0.0193	2.02
16,400	5	0.0278	0.0280	1.98
10,000	10	0.0339	0.0344	1.97
3,000	20	0.0203	0.0209	1.95
1,371	50	0.0232	0.0238	1.95
900	100	0.0305	0.0312	1.96

* electrode surface area = 0.98 cm²

TABLE III

APPARENT VALENCE OF ZINC DISSOLVING ANODICALLY IN 0.10 M
 KNO_3 + 0.30 M K_2SO_4 SOLUTION AT 25°C

Time (sec)	Current* (ma)	Wt. of Zinc		Apparent Valence
		Calcd. (g)	Expt. (g)	
58,500	1	0.0199	0.0200	1.99
13,600	5	0.0230	0.0235	1.96
9,700	10	0.0328	0.0338	1.94
2,000	20	0.0136	0.0145	1.91
1,400	50	0.0237	0.0250	1.89
1,170	100	0.0397	0.0421	1.88

TABLE IV

APPARENT VALENCE OF ZINC DISSOLVING ANODICALLY IN 0.30 M
 KNO_3 + 0.233 M K_2SO_4 SOLUTION AT 25°C

Time (sec)	Current* (ma)	Wt. of Zinc		Apparent Valence
		Calcd. (g)	Expt. (g)	
58,800	1	0.0198	0.0200	1.98
43,800	2.5	0.0371	0.0369	2.01
13,656	5	0.0231	0.0236	1.96
6,989	10	0.0237	0.0249	1.91
2,191	20	0.0148	0.0159	1.86
1,401	30	0.0143	0.0155	1.85
1,915	40	0.0259	0.0283	1.83
2,425	50	0.0411	0.0445	1.85
800	70	0.0190	0.0205	1.85
900	100	0.0305	0.0333	1.83
800	130	0.0352	0.0390	1.81
960	150	0.0489	0.0525	1.86

* electrode surface area = 0.98 cm²

TABLE V

APPARENT VALENCE OF ZINC DISSOLVING ANODICALLY IN 0.50 M
 $\text{KNO}_3 + 0.167 \text{ M K}_2\text{SO}_4$ SOLUTION AT 25°C

Time (sec)	Current* (ma)	Wt. of Zinc		Apparent Valence
		Calcd. (g)	Expt. (g)	
58,700	1	0.0199	0.0204	1.95
15,200	5	0.0257	0.0267	1.92
15,000	5	0.0254	0.0269	1.89
8,000	10	0.0271	0.0289	1.88
3,000	20	0.0204	0.0224	1.82
1,500	50	0.0254	0.0284	1.79
1,200	50	0.0203	0.0231	1.76
700	100	0.0237	0.0267	1.77

TABLE VI

APPARENT VALENCE OF ZINC DISSOLVING ANODICALLY IN 0.70 M
 $\text{KNO}_3 + 0.10 \text{ M K}_2\text{SO}_4$ SOLUTION AT 25°C

Time (sec)	Current* (ma)	Wt. of Zinc		Apparent Valence
		Calcd. (g)	Expt. (g)	
58,800	1	0.0199	0.0197	2.02
10,042	5	0.0172	0.0180	1.91
15,320	7	0.0364	0.0384	1.90
3,203	20	0.0217	0.0248	1.75
1,000	50	0.0170	0.0195	1.74
1,200	70	0.0284	0.0328	1.73
1,487	100	0.0504	0.0576	1.75

* electrode surface area = 0.98 cm^2

TABLE VII

APPARENT VALENCE OF ZINC DISSOLVING ANODICALLY IN 1.0 M
KNO₃ SOLUTION AT 25°C

Time (sec)	Current* (ma)	Wt. of Zinc		Apparent Valence
		Calcd. (g)	Expt. (g)	
58,500	1	0.0199	0.0200	1.99
10,000	5	0.0169	0.0181	1.87
9,000	10	0.0305	0.0340	1.79
1,400	30	0.0143	0.0167	1.71
1,600	50	0.0271	0.0321	1.69
900	100	0.0305	0.0360	1.69
800	150	0.0406	0.0497	1.64

TABLE VIII

APPARENT VALENCE OF ZINC DISSOLVING ANODICALLY IN 2.0 M
KNO₃ SOLUTION AT 25°C

Time (sec)	Current* (ma)	Wt. of Zinc		Apparent Valence
		Calcd. (g)	Expt. (g)	
81,000	1	0.0274	0.0278	1.97
10,393	5	0.0176	0.0192	1.84
7,000	10	0.0237	0.0271	1.75
6,700	15	0.0341	0.0380	1.72
3,245	50	0.0550	0.0665	1.65
1,154	100	0.0391	0.0470	1.66

* electrode surface area = 0.98 cm²

TABLE IX

APPARENT VALENCE OF ZINC DISSOLVING ANODICALLY IN 0.050 M
 $\text{KNO}_3 + 0.317 \text{ M K}_2\text{SO}_4$ SOLUTION AT 40°C

Time (sec)	Current* (ma)	Wt. of Zinc		Apparent Valence
		Calcd. (g)	Expt. (g)	
59,000	1	0.0200	0.0204	1.96
21,000	5	0.0355	0.0364	1.95
17,600	10	0.0596	0.0623	1.92
3,120	25	0.0264	0.0281	1.88
2,000	50	0.0339	0.0365	1.86

TABLE X

APPARENT VALENCE OF ZINC DISSOLVING ANODICALLY IN 0.10 M
 $\text{KNO}_3 + 0.30 \text{ M K}_2\text{SO}_4$ SOLUTION AT 40°C

Time (sec)	Current* (ma)	Wt. of Zinc		Apparent Valence
		Calcd. (g)	Expt. (g)	
55,800	1	0.0189	0.0193	1.96
14,201	5	0.0241	0.0248	1.94
18,670	5	0.0317	0.0328	1.93
11,400	10	0.0386	0.0406	1.90
4,000	15	0.0203	0.0215	1.89
3,010	30	0.0306	0.0336	1.82
1,810	50	0.0306	0.0336	1.82

* electrode surface area = 0.98 cm^2

TABLE XI

APPARENT VALENCE OF ZINC DISSOLVING ANODICALLY IN 0.50 M
 $\text{KNO}_3 + 0.167 \text{ M K}_2\text{SO}_4$ SOLUTION AT 40°C

Time (sec)	Current* (ma)	Wt. of Zinc		Apparent Valence
		Calcd. (g)	Expt. (g)	
65,000	1	0.0220	0.0228	1.93
12,400	5	0.0210	0.0222	1.89
4,280	15	0.0217	0.0245	1.77
3,410	25	0.0289	0.0336	1.72
1,340	50	0.0227	0.0267	1.70

TABLE XII

APPARENT VALENCE OF ZINC DISSOLVING ANODICALLY IN 1.0 M
 KNO_3 SOLUTION AT 40°C

Time (sec)	Current* (ma)	Wt. of Zinc		Apparent Valence
		Calcd. (g)	Expt. (g)	
58,500	1	0.0199	0.0211	1.89
10,400	5	0.0178	0.0192	1.83
11,420	10	0.0387	0.0436	1.77
4,000	15	0.0203	0.0238	1.71
3,210	30	0.0326	0.0408	1.60
1,660	50	0.0281	0.0355	1.58
1,600	50	0.0271	0.0340	1.59

* electrode surface area = 0.98 cm^2

TABLE XIII

APPARENT VALENCE OF ZINC DISSOLVING ANODICALLY IN 0.050 M
 $\text{KNO}_3 + 0.317 \text{ M K}_2\text{SO}_4$ SOLUTION AT 55°C

Time (sec)	Current* (ma)	Wt. of Zinc		Apparent Valence
		Calcd. (g)	Expt. (g)	
64,200	1	0.0217	0.0222	1.96
14,200	5	0.0240	0.0251	1.91
6,420	10	0.0217	0.0229	1.89
2,680	20	0.0182	0.0198	1.84
2,970	30	0.0302	0.0336	1.80
1,500	50	0.0255	0.0283	1.80
1,840	50	0.0311	0.0351	1.77

TABLE XIV

APPARENT VALENCE OF ZINC DISSOLVING ANODICALLY IN 0.10 M
 $\text{KNO}_3 + 0.30 \text{ M K}_2\text{SO}_4$ SOLUTION AT 55°C

Time (sec)	Current* (ma)	Wt. of Zinc		Apparent Valence
		Calcd. (g)	Expt. (g)	
59,210	1	0.0201	0.0208	1.93
16,210	5	0.0274	0.0294	1.87
7,100	10	0.0241	0.0262	1.84
3,710	20	0.0251	0.0281	1.79
2,500	35	0.0296	0.0343	1.73
1,920	50	0.0325	0.0376	1.73

* electrode surface area = 0.98 cm^2

TABLE XV

APPARENT VALENCE OF ZINC DISSOLVING ANODICALLY IN 0.50 M
 $\text{KNO}_3 + 0.167 \text{ M K}_2\text{SO}_4$ SOLUTION AT 55°C

Time (sec)	Current* (ma)	Wt. of Zinc		Apparent Valence
		Calcd. (g)	Expt. (g)	
67,240	1	0.0228	0.0238	1.91
18,891	5	0.0320	0.0346	1.85
9,120	10	0.0309	0.0345	1.79
4,406	15	0.0224	0.0265	1.69
2,910	30	0.0296	0.0358	1.65
1,910	50	0.0324	0.0397	1.63
2,875	50	0.0486	0.0610	1.59

TABLE XVI

APPARENT VALENCE OF ZINC DISSOLVING ANODICALLY IN 1.0 M
 KNO_3 SOLUTION AT 55°C

Time (sec)	Current* (ma)	Wt. of Zinc		Apparent Valence
		Calcd. (g)	Expt. (g)	
57,600	1	0.0194	0.0205	1.89
11,762	5	0.0199	0.0226	1.76
7,860	10	0.0266	0.0311	1.71
3,140	25	0.0266	0.0337	1.58
1,420	50	0.0240	0.0318	1.51
2,000	50	0.0339	0.0440	1.55

* electrode surface area = 0.98 cm^2

TABLE XVII

THE ANODIC POTENTIAL-CURRENT DENSITY RELATIONSHIP OF ZINC
DISSOLVING ANODICALLY IN 0.050 M KNO_3 + 0.317 M K_2SO_4
SOLUTION AT 25°C

Current [*] (ma)	Potential ^{**} (volts)	Current [*] (ma)	Potential ^{**} (volts)
0.0	-0.83	3.0	-0.68
0.1	-0.80	10.0	-0.65
0.3	-0.76	30.0	-0.56
1.0	-0.72	100.0	-0.38

TABLE XVIII

THE ANODIC POTENTIAL-CURRENT DENSITY RELATIONSHIP OF ZINC
DISSOLVING ANODICALLY IN 0.10 M KNO_3 + 0.30 M K_2SO_4
SOLUTION AT 25°C

Current [*] (ma)	Potential ^{**} (volts)	Current [*] (ma)	Potential ^{**} (volts)
0.0	-0.79	3.0	-0.66
0.1	-0.76	10.0	-0.63
0.3	-0.72	30.0	-0.56
1.0	-0.69	100.0	-0.30

* electrode surface area = 1.01 cm²

** normal hydrogen scale

TABLE XIX

THE ANODIC POTENTIAL-CURRENT DENSITY RELATIONSHIP OF ZINC DISSOLVING ANODICALLY IN 0.50 M KNO_3 + 0.167 M K_2SO_4 SOLUTION AT 25°C

Current [*] (ma)	Potential ^{**} (volts)	Current [*] (ma)	Potential ^{**} (volts)
0.0	-0.79	3.0	-0.64
0.1	-0.76	10.0	-0.61
0.3	-0.72	30.0	-0.55
1.0	-0.67	100.0	-0.37

TABLE XX

THE ANODIC POTENTIAL-CURRENT DENSITY RELATIONSHIP OF ZINC DISSOLVING ANODICALLY IN 1.0 M KNO_3 SOLUTION AT 25°C

Current [*] (ma)	Potential ^{**} (volts)	Current [*] (ma)	Potential ^{**} (volts)
0.0	-0.72	3.0	-0.58
0.1	-0.70	10.0	-0.53
0.3	-0.66	30.0	-0.41
1.0	-0.61	100.0	-0.18

* electrode surface area = 1.01 cm²

** normal hydrogen scale

TABLE XXI

THE ANODIC POTENTIAL-CURRENT DENSITY RELATIONSHIP OF ZINC
DISSOLVING ANODICALLY IN 0.050 M KNO_3 + 0.317 M K_2SO_4
SOLUTION AT 40°C

Current*	Potential**	Current*	Potential**
(ma)	(volts)	(ma)	(volts)
0.0	-0.81	3.0	-0.71
0.1	-0.80	10.0	-0.68
0.3	-0.78	30.0	-0.61
1.0	-0.74	100.0	-0.50

TABLE XXII

THE ANODIC POTENTIAL-CURRENT DENSITY RELATIONSHIP OF ZINC
DISSOLVING ANODICALLY IN 0.10 M KNO_3 + 0.30 M K_2SO_4
SOLUTION AT 40°C

Current*	Potential**	Current*	Potential**
(ma)	(volts)	(ma)	(volts)
0.0	-0.81	3.0	-0.70
0.1	-0.80	10.0	-0.66
0.3	-0.76	30.0	-0.60
1.0	-0.72	100.0	-0.42

* electrode surface area = 1.01 cm²

** normal hydrogen scale

TABLE XXIII

THE ANODIC POTENTIAL-CURRENT DENSITY RELATIONSHIP OF ZINC
DISSOLVING ANODICALLY IN 0.50 M KNO_3 + 0.167 M K_2SO_4
SOLUTION AT 40°C

Current*	Potential**	Current*	Potential**
(ma)	(volts)	(ma)	(volts)
0.0	-0.77	3.0	-0.67
0.1	-0.75	10.0	-0.64
0.3	-0.74	30.0	-0.58
1.0	-0.71	100.0	-0.53

TABLE XXIV

THE ANODIC POTENTIAL-CURRENT DENSITY RELATIONSHIP OF ZINC
DISSOLVING ANODICALLY IN 1.0 M KNO_3 SOLUTION AT 40°C

Current*	Potential**	Current*	Potential**
(ma)	(volts)	(ma)	(volts)
0.0	-0.73	3.0	-0.58
0.1	-0.71	10.0	-0.52
0.3	-0.68	30.0	-0.42
1.0	-0.63	100.0	-0.33

* electrode surface area = 1.01 cm²

** normal hydrogen scale

TABLE XXV

THE ANODIC POTENTIAL-CURRENT DENSITY RELATIONSHIP OF ZINC
DISSOLVING ANODICALLY IN 0.050 M KNO_3 + 0.317 M K_2SO_4
SOLUTION AT 55°C

Current [*] (ma)	Potential ^{**} (volts)	Current [*] (ma)	Potential ^{**} (volts)
0.0	-0.85	3.0	-0.73
0.1	-0.83	10.0	-0.70
0.3	-0.80	30.0	-0.64
1.0	-0.76	100.0	-0.51

TABLE XXVI

THE ANODIC POTENTIAL-CURRENT DENSITY RELATIONSHIP OF ZINC
DISSOLVING ANODICALLY IN 0.10 M KNO_3 + 0.30 M K_2SO_4
SOLUTION AT 55°C

Current [*] (ma)	Potential ^{**} (volts)	Current [*] (ma)	Potential ^{**} (volts)
0.0	-0.82	3.0	-0.73
0.1	-0.81	10.0	-0.68
0.3	-0.79	30.0	-0.62
1.0	-0.76	100.0	-0.52

* electrode surface area = 1.01 cm²

** normal hydrogen scale

TABLE XXVII

THE ANODIC POTENTIAL-CURRENT DENSITY RELATIONSHIP OF ZINC
DISSOLVING ANODICALLY IN 0.50 M KNO_3 + 0.167 M K_2SO_4
SOLUTION AT 55°C

Current [*] (ma)	Potential ^{**} (volts)	Current [*] (ma)	Potential ^{**} (volts)
0.0	-0.77	3.0	-0.66
0.1	-0.75	10.0	-0.63
0.3	-0.72	30.0	-0.54
1.0	-0.69	100.0	-0.28

TABLE XXVIII

THE ANODIC POTENTIAL-CURRENT DENSITY RELATIONSHIP OF ZINC
DISSOLVING ANODICALLY IN 1.0 M KNO_3 SOLUTION AT 55°C

Current [*] (ma)	Potential ^{**} (volts)	Current [*] (ma)	Potential ^{**} (volts)
0.0	-0.76	3.0	-0.62
0.1	-0.71	10.0	-0.57
0.3	-0.69	30.0	-0.40
1.0	-0.65	100.0	-0.24

* electrode surface area = 1.01 cm²

** normal hydrogen scale

TABLE XXIX

APPARENT VALENCE OF ZINC DISSOLVING ANODICALLY IN 0.23 M
 $K_2SO_4 + 0.10$ M $ZnCl_2$ SOLUTION

Temp. (°C)	Current* (ma)	Wt. of Zinc		Apparent Valence
		Calcd. (g)	Expt. (g)	
25	1	0.0208	0.02078	2.00
25	10	0.0345	0.03507	1.97
25	50	0.0307	0.03015	2.02
40	1	0.0241	0.02465	1.96
40	10	0.0336	0.03398	1.98
40	50	0.0318	0.03221	1.97
55	1	0.0227	0.02298	1.98
55	10	0.0338	0.03410	1.98
55	50	0.0344	0.03521	1.95

TABLE XXX

APPARENT VALENCE OF ZINC DISSOLVING ANODICALLY IN 0.23 M
 $K_2SO_4 + 0.10$ M $ZnBr_2$ SOLUTION

Temp. (°C)	Current* (ma)	Wt. of Zinc		Apparent Valence
		Calcd. (g)	Expt. (g)	
25	1	0.0199	0.02046	1.94
25	10	0.0333	0.03418	1.95
25	50	0.0332	0.03421	1.94
40	1	0.0217	0.02260	1.93
40	10	0.0338	0.03444	1.96
40	50	0.0457	0.04711	1.94
55	1	0.0225	0.02310	1.95
55	10	0.0353	0.03661	1.93
55	50	0.0350	0.03644	1.93

* electrode surface area = 1.01 cm^2

TABLE XXXI

APPARENT VALENCE OF ZINC DISSOLVING ANODICALLY IN 0.23 M
 $K_2SO_4 + 0.10 M ZnI_2$ SOLUTION

Temp. (°C)	Current* (ma)	Wt. of Zinc		Apparent Valence
		Calcd. (g)	Expt. (g)	
25	1	0.0241	0.02462	1.96
25	10	0.0328	0.03299	1.98
25	50	0.0266	0.02697	1.98
40	1	0.0229	0.02332	1.97
40	10	0.0341	0.03492	1.95
40	50	0.0335	0.03370	1.99
55	1	0.0241	0.02407	2.00
55	10	0.0327	0.03315	1.97
55	50	0.0336	0.03461	1.94

TABLE XXXII

APPARENT VALENCE OF ZINC DISSOLVING ANODICALLY IN 0.20 M
 $K_2SO_4 + 0.10 M ZnSO_4$ SOLUTION

Temp. (°C)	Current* (ma)	Wt. of Zinc		Apparent Valence
		Calcd. (g)	Expt. (g)	
25	1	0.0232	0.02314	2.01
25	10	0.0289	0.02941	1.97
25	50	0.0254	0.02564	1.99
40	1	0.0203	0.02073	1.96
40	10	0.0330	0.03279	2.02
40	50	0.0355	0.03594	1.98
55	1	0.0211	0.02091	2.02
55	10	0.0334	0.03410	1.96
55	50	0.0356	0.03551	2.01

* electrode surface area = 1.01 cm^2

TABLE XXXIII

APPARENT VALENCE OF ZINC DISSOLVING ANODICALLY IN 0.23 M
 $K_2SO_4 + 0.10 M Zn(C_2H_3O_2)_2$ SOLUTION

Temp. (°C)	Current* (ma)	Wt. of Zinc		Apparent Valence
		Calcd. (g)	Expt. (g)	
25	1	0.0208	0.02074	2.01
25	10	0.0308	0.03065	2.01
25	50	0.0285	0.02897	1.97
40	1	0.0223	0.02281	1.96
40	10	0.0330	0.03287	2.01
40	50	0.0340	0.03411	2.00
55	1	0.0247	0.02501	1.98
55	10	0.0331	0.03384	1.96
55	50	0.0328	0.03339	1.96

TABLE XXXIV

APPARENT VALENCE OF ZINC DISSOLVING ANODICALLY IN 0.23 M
 $K_2SO_4 + 0.10 M Zn(NO_3)_2$ SOLUTION

Temp. (°C)	Current* (ma)	Wt. of Zinc		Apparent Valence
		Calcd. (g)	Expt. (g)	
25	1	0.0258	0.02621	1.96
25	10	0.0297	0.03121	1.90
25	50	0.0356	0.03762	1.89
40	1	0.0229	0.02340	1.96
40	10	0.0352	0.03674	1.92
40	50	0.0339	0.03642	1.86
55	1	0.0236	0.02441	1.94
55	10	0.0352	0.03794	1.86
55	50	0.0331	0.03740	1.77

* electrode surface area = 1.01 cm^2

TABLE XXXV

APPARENT VALENCE OF ZINC DISSOLVING ANODICALLY 0.320 M
 $K_2SO_4 + 0.010 M ZnCl_2$ SOLUTION

Temp. (°C)	Current* (ma)	Wt. of Zinc		Apparent Valence
		Calcd. (g)	Expt. (g)	
25	1	0.0225	0.02241	2.01
25	10	0.0726	0.07268	2.00
25	50	0.0361	0.03598	2.00
40	1	0.0218	0.02174	2.00
40	10	0.0411	0.04172	1.97
40	50	0.0318	0.03212	1.98
55	1	0.0242	0.02422	2.00
55	10	0.0297	0.03011	1.97
55	50	0.0317	0.03231	1.96

TABLE XXXVI

APPARENT VALENCE OF ZINC DISSOLVING ANODICALLY IN 0.320 M
 $K_2SO_4 + 0.010 M ZnBr_2$ SOLUTION

Temp. (°C)	Current* (ma)	Wt. of Zinc		Apparent Valence
		Calcd. (g)	Expt. (g)	
25	1	0.0214	0.02128	2.01
25	10	0.0591	0.05981	1.98
25	50	0.0317	0.03188	1.98
40	1	0.0225	0.02261	1.99
40	10	0.0340	0.03411	2.00
40	50	0.0389	0.03925	1.98
55	1	0.0211	0.02136	1.98
55	10	0.0294	0.02965	1.98
55	50	0.0355	0.03608	1.97

* electrode surface area = 1.01 cm^2

TABLE XXXVII

APPARENT VALENCE OF ZINC DISSOLVING ANODICALLY IN 0.320 M
 K_2SO_4 + 0.010 M ZnI_2 SOLUTION

Temp. (°C)	Current* (ma)	Wt. of Zinc		Apparent Valence
		Calcd. (g)	Expt. (g)	
25	1	0.0229	0.02281	2.01
25	10	0.0564	0.05649	2.00
25	50	0.0803	0.08111	1.98
40	1	0.0218	0.02194	1.99
40	10	0.0337	0.03391	1.99
40	50	0.0338	0.03400	1.98
55	1	0.0269	0.02706	1.98
55	10	0.0481	0.04891	1.97
55	50	0.0362	0.03644	1.98

TABLE XXXVIII

APPARENT VALENCE OF ZINC DISSOLVING ANODICALLY IN 0.320 M
 K_2SO_4 + 0.010 M $ZnSO_4$ SOLUTION

Temp. (°C)	Current* (ma)	Wt. of Zinc		Apparent Valence
		Calcd. (g)	Expt. (g)	
25	1	0.0225	0.02219	2.02
25	10	0.0546	0.05508	1.98
25	50	0.0509	0.05114	2.00
40	1	0.0321	0.02299	2.01
40	10	0.0332	0.03304	2.01
40	50	0.0335	0.03381	1.98
55	1	0.0225	0.02243	2.00
55	10	0.0353	0.03581	1.97
55	50	0.0330	0.03361	1.96

* electrode surface area = 1.01 cm²

TABLE XXXIX

APPARENT VALENCE OF ZINC DISSOLVING ANODICALLY IN 0.320 M
 $K_2SO_4 + 0.010 M Zn(C_2H_3O_2)_2$ SOLUTION

Temp. (°C)	Current* (ma)	Wt. of Zinc		Apparent Valence
		Calcd. (g)	Expt. (g)	
25	1	0.0235	0.02330	2.02
25	10	0.0462	0.04565	2.02
25	50	0.0345	0.03463	1.99
40	1	0.0226	0.02282	1.98
40	10	0.0340	0.03434	1.98
40	50	0.0342	0.03451	1.98
55	1	0.0254	0.02536	2.00
55	10	0.0420	0.04255	1.98
55	50	0.0447	0.04541	1.97

TABLE XL

APPARENT VALENCE OF ZINC DISSOLVING ANODICALLY IN 0.320 M
 $K_2SO_4 + 0.010 M Zn(NO_3)_2$ SOLUTION

Temp. (°C)	Current* (ma)	Wt. of Zinc		Apparent Valence
		Calcd. (g)	Expt. (g)	
25	1	0.0218	0.02179	2.00
25	10	0.0319	0.03234	1.97
25	50	0.0300	0.03034	1.98
40	1	0.0218	0.02214	1.97
40	10	0.0339	0.03441	1.97
40	50	0.0339	0.03456	1.96
55	1	0.0225	0.02264	1.99
55	10	0.0353	0.05566	1.98
55	50	0.0358	0.03634	1.97

* electrode surface area = 1.01 cm²

TABLE XLI

THE ANODIC POTENTIAL-CURRENT DENSITY RELATIONSHIP OF ZINC DISSOLVING ANODICALLY IN 0.230 M K_2SO_4 + 0.10 M $ZnCl_2$ SOLUTION AT 25°C

Current [*] (ma)	Potential ^{**} (volts)	Current [*] (ma)	Potential ^{**} (volts)
0.0	-0.83	3.0	-0.79
0.1	-0.82	10.0	-0.77
0.3	-0.81	30.0	-0.72
1.0	-0.80	100.0	-0.54

TABLE XLII

THE ANODIC POTENTIAL-CURRENT DENSITY RELATIONSHIP OF ZINC DISSOLVING ANODICALLY IN 0.320 M K_2SO_4 + 0.010 M $ZnCl_2$ SOLUTION AT 25°C

Current [*] (ma)	Potential ^{**} (volts)	Current [*] (ma)	Potential ^{**} (volts)
0.0	-0.86	3.0	-0.82
0.1	-0.85	10.0	-0.80
0.3	-0.84	30.0	-0.76
1.0	-0.83	100.0	-0.63

* electrode surface area = 1.01 cm²

** normal hydrogen scale

TABLE XLIII

THE ANODIC POTENTIAL-CURRENT DENSITY RELATIONSHIP OF ZINC
DISSOLVING ANODICALLY IN 0.230 M K_2SO_4 + 0.10 M $ZnBr_2$
SOLUTION AT 25°C

Current [*] (ma)	Potential ^{**} (volts)	Current [*] (ma)	Potential ^{**} (volts)
0.0	-0.84	3.0	-0.81
0.1	-0.83	10.0	-0.79
0.3	-0.82	30.0	-0.74
1.0	-0.82	100.0	-0.56

TABLE XLIV

THE ANODIC POTENTIAL-CURRENT DENSITY RELATIONSHIP OF ZINC
DISSOLVING ANODICALLY IN 0.320 M K_2SO_4 + 0.010 M $ZnBr_2$
SOLUTION AT 25°C

Current [*] (ma)	Potential ^{**} (volts)	Current [*] (ma)	Potential ^{**} (volts)
0.0	-0.86	3.0	-0.77
0.1	-0.84	10.0	-0.74
0.3	-0.82	30.0	-0.70
1.0	-0.80	100.0	-0.57

* electrode surface area = 1.01 cm²

** normal hydrogen scale

TABLE XLV

THE ANODIC POTENTIAL-CURRENT DENSITY RELATIONSHIP OF ZINC
DISSOLVING ANODICALLY IN 0.230 M K_2SO_4 + 0.10 M ZnI_2
SOLUTION AT 25°C

Current [*] (ma)	Potential ^{**} (volts)	Current [*] (ma)	Potential ^{**} (volts)
0.0	-0.72	3.0	-0.69
0.1	-0.71	10.0	-0.68
0.3	-0.70	30.0	-0.64
1.0	-0.70	100.0	-0.53

TABLE XLVI

THE ANODIC POTENTIAL-CURRENT DENSITY RELATIONSHIP OF ZINC
DISSOLVING ANODICALLY IN 0.320 M K_2SO_4 + 0.010 M ZnI_2
SOLUTION AT 25°C

Current [*] (ma)	Potential ^{**} (volts)	Current [*] (ma)	Potential ^{**} (volts)
0.0	-0.86	3.0	-0.82
0.1	-0.85	10.0	-0.80
0.3	-0.84	30.0	-0.76
1.0	-0.83	100.0	-0.63

* electrode surface area = 1.01 cm²

** normal hydrogen scale

TABLE XLVII

THE ANODIC POTENTIAL-CURRENT DENSITY RELATIONSHIP OF ZINC
DISSOLVING ANODICALLY IN 0.20 M K_2SO_4 + 0.10 M $ZnSO_4$
SOLUTION AT 25°C

Current [*] (ma)	Potential ^{**} (volts)	Current [*] (ma)	Potential ^{**} (volts)
0.0	-0.80	3.0	-0.76
0.1	-0.79	10.0	-0.75
0.3	-0.78	30.0	-0.73
1.0	-0.77	100.0	-0.61

TABLE XLVIII

THE ANODIC POTENTIAL-CURRENT DENSITY RELATIONSHIP OF ZINC
DISSOLVING ANODICALLY IN 0.320 M K_2SO_4 + 0.010 M $ZnSO_4$
SOLUTION AT 25°C

Current [*] (ma)	Potential ^{**} (volts)	Current [*] (ma)	Potential ^{**} (volts)
0.0	-0.82	3.0	-0.77
0.1	-0.81	10.0	-0.75
0.3	-0.80	30.0	-0.70
1.0	-0.79	100.0	-0.62

* electrode surface area = 1.01 cm²

** normal hydrogen scale

TABLE II

THE ANODIC POTENTIAL-CURRENT DENSITY RELATIONSHIP OF ZINC DISSOLVING ANODICALLY IN 0.230 M K_2SO_4 + 0.10 M $Zn(C_2H_3O_2)_2$ SOLUTION AT 25°C

Current [*] (ma)	Potential ^{**} (volts)	Current [*] (ma)	Potential ^{**} (volts)
0.0	-0.84	3.0	-0.80
0.1	-0.83	10.0	-0.78
0.3	-0.82	30.0	-0.72
1.0	-0.81	100.0	-0.46

TABLE I

THE ANODIC POTENTIAL-CURRENT DENSITY RELATIONSHIP OF ZINC DISSOLVING ANODICALLY IN 0.320 M K_2SO_4 + 0.010 M $Zn(C_2H_3O_2)_2$ SOLUTION AT 25°C

Current [*] (ma)	Potential ^{**} (volts)	Current [*] (ma)	Potential ^{**} (volts)
0.0	-0.87	3.0	-0.82
0.1	-0.86	10.0	-0.80
0.3	-0.85	30.0	-0.73
1.0	-0.84	100.0	-0.56

* electrode surface area = 1.01 cm²

** normal hydrogen scale

TABLE LI

THE ANODIC POTENTIAL-CURRENT DENSITY RELATIONSHIP OF ZINC DISSOLVING ANODICALLY IN 0.230 M K_2SO_4 + 0.10 M $Zn(NO_3)_2$ SOLUTION AT 25°C

Current [*] (ma)	Potential ^{**} (volts)	Current [*] (ma)	Potential ^{**} (volts)
0.0	-0.79	3.0	-0.66
0.1	-0.77	10.0	-0.62
0.3	-0.74	30.0	-0.56
1.0	-0.72	100.0	-0.31

TABLE LII

THE ANODIC POTENTIAL-CURRENT DENSITY RELATIONSHIP OF ZINC DISSOLVING ANODICALLY IN 0.320 M K_2SO_4 + 0.010 M $Zn(NO_3)_2$ SOLUTION AT 25°C

Current [*] (ma)	Potential ^{**} (volts)	Current [*] (ma)	Potential ^{**} (volts)
0.0	-0.83	3.0	-0.76
0.1	-0.78	10.0	-0.75
0.3	-0.77	30.0	-0.69
1.0	-0.76	100.0	-0.55

* electrode surface area = 1.01 cm²

** normal hydrogen scale

TABLE LIII

THE ANODIC POTENTIAL-CURRENT DENSITY RELATIONSHIP OF ZINC DISSOLVING ANODICALLY IN 0.230 M K_2SO_4 + 0.10 M $ZnCl_2$ SOLUTION AT 40°C

Current [*] (ma)	Potential ^{**} (volts)	Current [*] (ma)	Potential ^{**} (volts)
0.0	-0.84	3.0	-0.80
0.1	-0.83	10.0	-0.78
0.3	-0.82	30.0	-0.75
1.0	-0.81	100.0	-0.59

TABLE LIV

THE ANODIC POTENTIAL-CURRENT DENSITY RELATIONSHIP OF ZINC DISSOLVING ANODICALLY IN 0.320 M K_2SO_4 + 0.010 M $ZnCl_2$ SOLUTION AT 40°C

Current [*] (ma)	Potential ^{**} (volts)	Current [*] (ma)	Potential ^{**} (volts)
0.0	-0.87	3.0	-0.84
0.1	-0.87	10.0	-0.81
0.3	-0.86	30.0	-0.76
1.0	-0.85	100.0	-0.63

* electrode surface area = 1.01 cm²

** normal hydrogen scale

TABLE LV

THE ANODIC POTENTIAL-CURRENT DENSITY RELATIONSHIP OF ZINC
DISSOLVING ANODICALLY IN 0.230 M K_2SO_4 + 0.10 M $ZnBr_2$
SOLUTION AT 40°C

Current*	Potential**	Current*	Potential**
(ma)	(volts)	(ma)	(volts)
0.0	-0.83	3.0	-0.80
0.1	-0.82	10.0	-0.79
0.3	-0.81	30.0	-0.75
1.0	-0.81	100.0	-0.62

TABLE LVI

THE ANODIC POTENTIAL-CURRENT DENSITY RELATIONSHIP OF ZINC
DISSOLVING ANODICALLY IN 0.320 M K_2SO_4 + 0.010 M $ZnBr_2$
SOLUTION AT 40°C

Current*	Potential**	Current*	Potential**
(ma)	(volts)	(ma)	(volts)
0.0	-0.87	3.0	-0.83
0.1	-0.86	10.0	-0.81
0.3	-0.85	30.0	-0.77
1.0	-0.84	100.0	-0.68

* electrode surface area = 1.01 cm²

** normal hydrogen scale

TABLE LVII

THE ANODIC POTENTIAL-CURRENT DENSITY RELATIONSHIP OF ZINC
DISSOLVING ANODICALLY IN 0.230 M K_2SO_4 + 0.10 M ZnI_2
SOLUTION AT 40°C

Current [*] (ma)	Potential ^{**} (volts)	Current [*] (ma)	Potential ^{**} (volts)
0.0	-0.84	3.0	-0.79
0.1	-0.81	10.0	-0.78
0.3	-0.80	30.0	-0.76
1.0	-0.80	100.0	-0.67

TABLE LVIII

THE ANODIC POTENTIAL-CURRENT DENSITY RELATIONSHIP OF ZINC
DISSOLVING ANODICALLY IN 0.320 M K_2SO_4 + 0.010 M ZnI_2
SOLUTION AT 40°C

Current [*] (ma)	Potential ^{**} (volts)	Current [*] (ma)	Potential ^{**} (volts)
0.0	-0.86	3.0	-0.83
0.1	-0.85	10.0	-0.81
0.3	-0.85	30.0	-0.74
1.0	-0.84	100.0	-0.56

* electrode surface area = 1.01 cm²

** normal hydrogen scale

TABLE LIX

THE ANODIC POTENTIAL-CURRENT DENSITY RELATIONSHIP OF ZINC
DISSOLVING ANODICALLY IN 0.20 M K_2SO_4 + 0.10 M $ZnSO_4$
SOLUTION AT 40°C

Current [*] (ma)	Potential ^{**} (volts)	Current [*] (ma)	Potential ^{**} (volts)
0.0	-0.84	3.0	-0.81
0.1	-0.83	10.0	-0.79
0.3	-0.83	30.0	-0.75
1.0	-0.82	100.0	-0.59

TABLE LX

THE ANODIC POTENTIAL-CURRENT DENSITY RELATIONSHIP OF ZINC
DISSOLVING ANODICALLY IN 0.320 M K_2SO_4 + 0.010 M $ZnSO_4$
SOLUTION AT 40°C

Current [*] (ma)	Potential ^{**} (volts)	Current [*] (ma)	Potential ^{**} (volts)
0.0	-0.87	3.0	-0.83
0.1	-0.86	10.0	-0.81
0.3	-0.85	30.0	-0.77
1.0	-0.84	100.0	-0.68

* electrode surface area = 1.01 cm²

** normal hydrogen scale

TABLE LXI

THE ANODIC POTENTIAL-CURRENT DENSITY RELATIONSHIP OF ZINC DISSOLVING ANODICALLY IN 0.230 M K_2SO_4 + 0.10 M $Zn(C_2H_3O_2)_2$ SOLUTION AT 40°C

Current [*] (ma)	Potential ^{**} (volts)	Current [*] (ma)	Potential ^{**} (volts)
0.0	-0.81	3.0	-0.78
0.1	-0.80	10.0	-0.77
0.3	-0.80	30.0	-0.73
1.0	-0.79	100.0	-0.55

TABLE LXII

THE ANODIC POTENTIAL-CURRENT DENSITY RELATIONSHIP OF ZINC DISSOLVING ANODICALLY IN 0.320 M K_2SO_4 + 0.010 M $Zn(C_2H_3O_2)_2$ SOLUTION AT 40°C

Current [*] (ma)	Potential ^{**} (volts)	Current [*] (ma)	Potential ^{**} (volts)
0.0	-0.87	3.0	-0.83
0.1	-0.86	10.0	-0.81
0.3	-0.85	30.0	-0.75
1.0	-0.84	100.0	-0.62

* electrode surface area = 1.01 cm²

** normal hydrogen scale

TABLE LXIII

THE ANODIC POTENTIAL-CURRENT DENSITY RELATIONSHIP OF ZINC DISSOLVING ANODICALLY IN 0.230 M K_2SO_4 + 0.10 M $Zn(NO_3)_2$ SOLUTION AT 40°C

Current [*] (ma)	Potential ^{**} (volts)	Current [*] (ma)	Potential ^{**} (volts)
0.0	-0.79	3.0	-0.69
0.1	-0.78	10.0	-0.64
0.3	-0.76	30.0	-0.58
1.0	-0.72	100.0	-0.40

TABLE LXIV

THE ANODIC POTENTIAL-CURRENT DENSITY RELATIONSHIP OF ZINC DISSOLVING ANODICALLY IN 0.320 M K_2SO_4 + 0.010 M $Zn(NO_3)_2$ SOLUTION AT 40°C

Current [*] (ma)	Potential ^{**} (volts)	Current [*] (ma)	Potential ^{**} (volts)
0.0	-0.84	3.0	-0.75
0.1	-0.82	10.0	-0.73
0.3	-0.80	30.0	-0.68
1.0	-0.78	100.0	-0.50

* electrode surface area = 1.01 cm²

** normal hydrogen scale

TABLE LXV

THE ANODIC POTENTIAL-CURRENT DENSITY RELATIONSHIP OF ZINC
DISSOLVING ANODICALLY IN 0.230 M K_2SO_4 + 0.10 M $ZnCl_2$
SOLUTION AT 55°C

Current [*] (ma)	Potential ^{**} (volts)	Current [*] (ma)	Potential ^{**} (volts)
0.0	-0.82	3.0	-0.79
0.1	-0.81	10.0	-0.78
0.3	-0.81	30.0	-0.75
1.0	-0.80	100.0	-0.65

TABLE LXVI

THE ANODIC POTENTIAL-CURRENT DENSITY RELATIONSHIP OF ZINC
DISSOLVING ANODICALLY IN 0.320 M K_2SO_4 + 0.010 M $ZnCl_2$
SOLUTION AT 55°C

Current [*] (ma)	Potential ^{**} (volts)	Current [*] (ma)	Potential ^{**} (volts)
0.0	-0.87	3.0	-0.84
0.1	-0.86	10.0	-0.82
0.3	-0.86	30.0	-0.78
1.0	-0.85	100.0	-0.72

* electrode surface area = 1.01 cm²

** normal hydrogen scale

TABLE LXVII

THE ANODIC POTENTIAL-CURRENT DENSITY RELATIONSHIP OF ZINC
DISSOLVING ANODICALLY IN 0.230 M K_2SO_4 + 0.10 M $ZnBr_2$
SOLUTION AT 55°C

Current [*] (ma)	Potential ^{**} (volts)	Current [*] (ma)	Potential ^{**} (volts)
0.0	-0.84	3.0	-0.80
0.1	-0.83	10.0	-0.79
0.3	-0.82	30.0	-0.77
1.0	-0.81	100.0	-0.63

TABLE LXVIII

THE ANODIC POTENTIAL-CURRENT DENSITY RELATIONSHIP OF ZINC
DISSOLVING ANODICALLY IN 0.320 M K_2SO_4 + 0.010 M $ZnBr_2$
SOLUTION AT 55°C

Current [*] (ma)	Potential ^{**} (volts)	Current [*] (ma)	Potential ^{**} (volts)
0.0	-0.86	3.0	-0.82
0.1	-0.85	10.0	-0.81
0.3	-0.84	30.0	-0.76
1.0	-0.83	100.0	-0.66

* electrode surface area = 1.01 cm²

** normal hydrogen scale

TABLE LXIX

THE ANODIC POTENTIAL-CURRENT DENSITY RELATIONSHIP OF ZINC
DISSOLVING ANODICALLY IN 0.230 M K_2SO_4 + 0.10 M ZnI_2
SOLUTION AT 55°C

Current*	Potential**	Current*	Potential**
(ma)	(volts)	(ma)	(volts)
0.0	-0.83	3.0	-0.80
0.1	-0.82	10.0	-0.80
0.3	-0.82	30.0	-0.78
1.0	-0.81	100.0	-0.73

TABLE LXX

THE ANODIC POTENTIAL-CURRENT DENSITY RELATIONSHIP OF ZINC
DISSOLVING ANODICALLY IN 0.320 M K_2SO_4 + 0.010 M ZnI_2
SOLUTION AT 55°C

Current*	Potential**	Current*	Potential**
(ma)	(volts)	(ma)	(volts)
0.0	-0.86	3.0	-0.83
0.1	-0.86	10.0	-0.81
0.3	-0.85	30.0	-0.79
1.0	-0.84	100.0	-0.73

* electrode surface area = 1.01 cm²

** normal hydrogen scale

TABLE LXXI

THE ANODIC POTENTIAL-CURRENT DENSITY RELATIONSHIP OF ZINC
DISSOLVING ANODICALLY IN 0.20 M K_2SO_4 + 0.10 M $ZnSO_4$
SOLUTION AT 55°C

Current [*] (ma)	Potential ^{**} (volts)	Current [*] (ma)	Potential ^{**} (volts)
0.0	-0.81	3.0	-0.78
0.1	-0.80	10.0	-0.77
0.3	-0.79	30.0	-0.71
1.0	-0.79	100.0	-0.55

TABLE LXXII

THE ANODIC POTENTIAL-CURRENT DENSITY RELATIONSHIP OF ZINC
DISSOLVING ANODICALLY IN 0.320 M K_2SO_4 + 0.010 M $ZnSO_4$
SOLUTION AT 55°C

Current [*] (ma)	Potential ^{**} (volts)	Current [*] (ma)	Potential ^{**} (volts)
0.0	-0.84	3.0	-0.81
0.1	-0.83	10.0	-0.79
0.3	-0.83	30.0	-0.73
1.0	-0.82	100.0	-0.59

* electrode surface area = 1.01 cm²

** normal hydrogen scale

TABLE LXXIII

THE ANODIC POTENTIAL-CURRENT DENSITY RELATIONSHIP OF ZINC DISSOLVING ANODICALLY IN 0.230 M K_2SO_4 + 0.10 M $Zn(C_2H_3O_2)_2$ SOLUTION AT 55°C

Current [*] (ma)	Potential ^{**} (volts)	Current [*] (ma)	Potential ^{**} (volts)
0.0	-0.83	3.0	-0.80
0.1	-0.82	10.0	-0.79
0.3	-0.81	30.0	-0.74
1.0	-0.81	100.0	-0.48

TABLE LXXIV

THE ANODIC POTENTIAL-CURRENT DENSITY RELATIONSHIP OF ZINC DISSOLVING ANODICALLY IN 0.320 M K_2SO_4 + 0.010 M $Zn(C_2H_3O_2)_2$ SOLUTION AT 55°C

Current [*] (ma)	Potential ^{**} (volts)	Current [*] (ma)	Potential ^{**} (volts)
0.0	-0.87	3.0	-0.84
0.1	-0.86	10.0	-0.82
0.3	-0.86	30.0	-0.79
1.0	-0.85	100.0	-0.70

* electrode surface area = 1.01 cm²

** normal hydrogen scale

TABLE LXXV

THE ANODIC POTENTIAL-CURRENT DENSITY RELATIONSHIP OF ZINC DISSOLVING ANODICALLY IN 0.230 M K_2SO_4 + 0.10 M $Zn(NO_3)_2$ SOLUTION AT 55°C

Current*	Potential**	Current*	Potential**
(ma)	(volts)	(ma)	(volts)
0.0	-0.85	3.0	-0.71
0.1	-0.83	10.0	-0.66
0.3	-0.79	30.0	-0.60
1.0	-0.75	100.0	-0.43

TABLE LXXVI

THE ANODIC POTENTIAL-CURRENT DENSITY RELATIONSHIP OF ZINC DISSOLVING ANODICALLY IN 0.320 M K_2SO_4 + 0.010 M $Zn(NO_3)_2$ SOLUTION AT 55°C

Current*	Potential**	Current*	Potential**
(ma)	(volts)	(ma)	(volts)
0.0	-0.85	3.0	-0.74
0.1	-0.82	10.0	-0.72
0.3	-0.79	30.0	-0.67
1.0	-0.77	100.0	-0.46

* electrode surface area = 1.01 cm²

** normal hydrogen scale

VITA

Sun, Yun-chung was born on February 18, 1937, in Shanton, China, as the first son of Mr. and Mrs. Sun, Shao-yang. In 1949 he migrated to Taipei, Taiwan, where he finished his elementary school studies and attended Taiwan Provincial Fu-chung High School. In 1957, he entered Tunghai University, receiving a Bachelor of Science degree in Chemical Engineering in June of 1961. After graduation, he served in the Chinese Marine Corps for one year of military service as a second lieutenant.

In January, 1963 he came to the United States to attend the University of Missouri at Rolla for advanced studies, where he received the Master of Science degree in Chemical Engineering in May of 1964.

He held a Graduate Teaching Assistantship in Chemistry during the three semesters of his enrollment while pursuing studies to the Master of Science degree. He received a Space Sciences Research Fellowship during his continuous studies for the degree of Doctor of Philosophy in Chemical Engineering.